THE UNIVERSITY OF OKLAHOMA

GRADUATE COLLEGE

LINEARIZED BUOYANT MOTION IN A CLOSED CONTAINER

A DISSERTATION

SUBMITTED TO THE GRADUATE FACULTY

in partial fulfillment of the requirements for the

degree of

DOCTOR OF PHILOSOPHY

BY

ROBERT THOMAS DOTY

Norman, Oklahoma

1973

LINEARIZED BUOYANT MOTION IN A CLOSED CONTAINER

APPROVED BY

Martin C. Hyclibee

M. Rasmussen

C. M. Shepherd

Robin E. Tennant

DISSERTATION COMMITTEE

ACKNOWLEDGMENTS

My deepest thanks go to Dr. Martin C. Jischke for serving as chairman of my doctoral advisory committee. Without his initial efforts and suggestions, as well as his many technical contributions throughout the past year, this dissertation could not have been completed. Yet his support extended beyond mere technical assistance. The inspiration and encouragement he gave me throughout my graduate program and the example he set, both in and out of the classroom, gave me hope when things seemed hopeless.

I would like to thank my very patient and understanding wife Rieta, without whom the past four years would not have been worthwhile.

ABSTRACT

The linearized set of equations that govern the thermally-driven natural convection flow of a Newtonian fluid are developed in a rational manner and the approximations involved are explicitly described. An arbitrarily shaped closed container completely filled with this "Boussinesq" fluid is considered. It is assumed that the fluid is originally in some physically permissible stable state of rest and that at an initial instant the temperature of the container is impulsively changed. The ensuing unsteady laminar motion is found by solving the linearized equations. A "boundary-layer, inviscid-interior" decomposition leads to a modified asymptotic expansion scheme of analysis. The boundary-layer concept is valid only for sufficiently large values of the Grashof number. Thus, we restrict our attention to this practically important flow regime and, in addition, limit Prandtl number to order unity.

It is found that the inviscid interior region responds to a special "average" value of the temperature perturbation. The effect of the boundary layer is to smear out, or average, any circumferential variation in this perturbation so that the interior, in effect, responds to an isothermal boundary in each horizontal plane. The temperature and vertical velocity component are expressed simply in terms of this "average" container temperature. The horizontal velocity potential is governed by a Poisson equation whose general solution is developed in terms of a Neumann function that depends on the container geometry. Several specific examples are solved to illustrate the nature of the flow.

TABLE OF CONTENTS

	Page
ACKNOWLEDGMENTS	iii
ABSTRACT	iv
LIST OF ILLUSTRATIONS	vii
NOMENCLATURE	ix
Chapter	
I. INTRODUCTION	1
Motivation	1
Earlier Work	5
Method of Attack	11
II. THEORETICAL DEVELOPMENT	16
Governing Equations	16
Static Basic State	17
Weak Stratification	18
Nondimensional Equations	21
Small Disturbances	22
Linearized Equations	23
Perturbation Expansion	29
Problem Sequence	33
III. ANALYSIS	36
Zeroth-Order Interior	36
First-Order Boundary Layer	36

TABLE OF CONTENTS (Cont'd.)

First-Order Interior. 41

Remarks 50

IV. APPLICATION OF THE THEORY 52

Preliminary Remarks 52

Right Cylinders 57

Circular Cross Section 59

z-Dependent Boundary Condition 61

Azimuthally Varying Boundary Condition . . . 66

Elliptical Cross Section 72

Ellipsoid of Revolution 76

V. CONCLUSIONS AND RECOMMENDATIONS 83

Conclusions 83

Recommendations for Future Research 87

REFERENCES 91

APPENDIX 94

LEIBNITZ'S RULE FOR THE CROSS PLANE 94

LIST OF ILLUSTRATIONS

Figure		Page
2.1	The Basic State and Container Geometry.	19
2.2	A Typical Temperature Perturbation Leading to Linearized Flow	28
3.1	Cross-Plane Geometry and Unit Vectors	39
3.2	Surface Integral Geometry	46
4.1	Heat-Up Geometry.	53
4.2	Cross-Plane Geometry.	56
4.3	Right Cylinder.	58
4.4	Right Circular Cylinder	60
4.5	General Linear Boundary Condition	63
4.6	Linear Boundary Temperature Producing Zero Boundary-Layer Suction.	65
4.7	Linear Boundary Temperature Producing Four-Cell Flow.	67
4.8	Azimuthally-Varying Boundary Temperature Producing Plugged Flow.	69
4.9	Azimuthally-Varying Boundary Temperature Producing Four-Cell Flow.	71
4.10	Right Elliptical Cylinder	73
4.11	Cross-Flow Streamlines for a Right Elliptical Cylinder	77

LIST OF ILLUSTRATIONS (Cont'd.)

4.12	Ellipsoid of Revolution.	78
4.13	Heat-up Comparison Between a Cylinder and an Ellipsoid	81
5.1	Interior Heat-up Mechanism	85
A.1	Cross-Plane Geometry	96
A.2	Rigid Cylinder and Unit Normals.	97

NOMENCLATURE

a	semi-major axis (elliptical cylinder)
a	cross-plane radius (ellipsoid of revolution)
A	cross-plane area (nondimensionalized)
$\bar{A}$	parameter, see Eq. (4.57)
b	semi-minor axis (elliptical cylinder)
c_p	specific heat at constant pressure (fluid)
$\mathcal{C}_\varphi$	cross-plane perimeter (nondimensionalized)
$\hat{e}_r$	unit vector in radial direction (cylindrical coordinate system)
$\hat{e}_T$	unit vector tangent to $\mathcal{C}_\varphi$
$\hat{e}_z$	unit vector in vertical direction (opposing gravity)
$\hat{e}_1, \hat{e}_2$	general cross-plane unit vectors
$f(\tau)$	function of integration, see Eq. (3.48)
$f(x,y)$	two-dimensional function defining the container, see Eq. (A.6)
$f(z)$	z-dependence of azimuthally varying container temperature, see Eq. (4.35)
$F(x,y,z)$	three-dimensional function defining the container, see Eq. (A.6)
g	gravitational constant
$g(z)$	function of integration, see Eq. (3.49)
h	height of rigid cylinder

NOMENCLATURE (Cont'd.)

h_1, h_2	general cross-plane scale factors
H(t)	Heaviside step function
k	thermal conductivity of fluid
L	container height
m	slope of linear temperature profile, see Eq. (4.34)
$\hat{n}$	unit vector normal to the container
$\hat{n}^*$	unit vector normal to the container in the cross plane
$\hat{n}_T, \hat{n}_B$	unit vector normal to top and bottom of rigid cylinder respectively
N	Neumann function, see Eq. (4.45)
p	fluid pressure
Q	arbitrary quantity
r	radial coordinate (cylindrical coordinate system)
$\vec{r}$	position vector
R	radius of circular cylinder
R(t)	arbitrary three-dimensional region, see Eq. (A.1)
S(t)	three-dimensional closed surface, see Eq. (A.1)
t	time
T	fluid temperature
u,v	general cross-plane velocity components
U,V	elliptic coordinates (elliptic cylindrical coordinate system)
$\vec{v}$	cross-plane velocity
$\vec{V}$	total fluid velocity
W	vertical component of fluid velocity
X_1, X_2	general cross-plane coordinates

z	vertical spatial coordinate

Greek Letters

α	frequency of azimuthally varying container temperature, see Eq. (4.35)
β	coefficient of thermal expansion, see Eq. (2.6)
ΔT	basic temperature change across the container (in the vertical direction)
ϵ	temperature perturbation parameter
$\overleftrightarrow{\epsilon}$	rate-of-strain tensor
$\vec{\zeta}$	position vector to a field point
θ	azimuthal coordinate (cylindrical coordinate system)
$\varkappa$	coefficient of isothermal compression, see Eq. (2.7)
λ	second coefficient of viscosity
μ	first coefficient of viscosity
ξ	boundary-layer coordinate
ξ^*	rescaled boundary-layer coordinate, see Eq. (3.13)
ρ	fluid density
Σ	container
Σ_T	portion of the container above $\mathcal{G}$
τ	heat-up time scale, see Eq. (2.77), nondimensional
$\overleftrightarrow{\tau}$	viscous stress tensor
τ_H	heat-up time (e-folding time), nondimensional
φ	cross-plane velocity potential
$\vec{\omega}$	vorticity

Nondimensional Parameters

G_r	Grashof number, $(\rho_{op}^2 \, g \, L^3 \beta_{op} \Delta T/\mu^2)$
M	compressibility factor, $(\beta_{op} T_{op} \, g \, L/c_{p_{op}} \Delta T)$
N	Brunt-Väisälä frequency, $\sqrt{\frac{g}{L} \beta_{op} \Delta T}$
P_r	Prandtl number, $(\mu \, c_{p_{op}}/k)$
R_a	Rayleigh number, $P_r G_r$

Subscripts

B	basic-state value (unperturbed state)
op	operating value (value of basic state at container bottom)
ref	reference value (dimensional)
REP	representative value, see Eq. (2.13)
Σ	value on the container
0	zeroth-order term (order unity term)
1	first-order term (order $R_a^{-\frac{1}{4}}$ term)

Superscripts

*	nondimensional perturbation variable
+	rescaled nondimensional perturbation variable, see Eq. (2.58) through Eq. (2.62)

Abbreviations

LNG	liquified natural gas
LOX	liquid oxygen

STP	standard temperature and pressure

Mathematical Symbols

D	substantial (material) derivative operator
∇	gradient operator
∇_2	two-dimensional gradient operator in the cross plane, see Eq. (4.8)
∇^2	Laplacian operator
∇_2^2	two-dimensional Laplacian operator, see Eq. (4.9)
$\overleftrightarrow{\Pi}$	unit tensor (metric tensor)
$( )^+$	conjugate tensor
$( )'$	ordinary derivative
$\tilde{( )}$	boundary-layer variable
$< >$	average value, see Eq. (4.1)
$\{$	indicates boundary condition

LINEARIZED BUOYANT MOTION IN A CLOSED CONTAINER

CHAPTER I

INTRODUCTION

Motivation

Many engineering problems have arisen within the past fifteen years in which unsteady buoyancy-driven flows apparently play a central role. These problems can generally be classified as either "external" problems, such as the flow around a heated rod or plate in an otherwise quiescent fluid, or "internal" problems, such as the flow between parallel plates or in fluid-filled cavities.

As pointed out by Ostrach [1], the external problems have received a great deal of attention while relatively little has been done about internal problems thus far. Ostrach contends that the reason for this is not the greater importance of the external problem but rather that internal natural convection problems are considerably more complex. This is because those external natural convection problems for which the Rayleigh number is large can be analyzed by the usual Prandtl boundary-layer theory that is so helpful in other external fluid flow problems. This is due to the assumption that the region exterior to the boundary layer can be assumed to be unaffected by the boundary layer in an external problem. For confined natural convection problems, on the other hand, a boundary layer will exist near the walls (for sufficiently large Rayleigh number)

but the region exterior to the boundary layer cannot be assumed to be independent of the boundary layer. In other words, the region exterior to the boundary layer will be completely enclosed by the boundary layer and will form a core region that is greatly affected by the boundary-layer behavior. Hence, the boundary layer and core are closely coupled to each other and this coupling constitutes the main source of difficulty in obtaining analytic solutions to internal problems.

We shall briefly describe some examples of contained natural convection flows in order to indicate the nature of the problem in general, the diversity of the specific applications, and the importance attached to the solution of these specific problems.

The first example in which buoyancy-driven flows play a central role deals with the storage of liquified natural gas (LNG). With the rapidly growing consumption of LNG as a low sulfur content fuel, the need for storage of large quantities of LNG has arisen. Large, land-based, cylindrical tanks (typically one hundred feet tall and three hundred feet wide) have been constructed for this purpose. Although the tanks are insulated, heating by solar radiation leads to LNG stratification and vaporization with attendant pressure build-up in the container. Periodically, this pressure must be relieved by venting to the atmosphere and thus LNG is lost. This loss of LNG by vaporization is critical to the economics of long term storage such as is involved in peak shaving operations. Further, at high vaporization rates, the dense LNG vapor flows along the ground, dispersing very slowly and causing a serious fire hazard. At present, we are unable to predict vaporization rate as a function of imposed heating rate, tank geometry and fluid properties

because the stratification is intimately coupled with the induced fluid motion in the tank.

The manufacture of glass represents a second area in which buoyancy-driven flows are of central interest. Glass is normally produced in open-hearth furnaces in which the glass ingredients are flame heated from above to form a melt. The raw materials (batch) are fed at one end of the furnace and float on the surface to form the so-called "batch heap" or cover. The charge reacts, is mixed by buoyancy-driven convection and by diffusion, and the product glass is withdrawn at the opposite end of the furnace. A full understanding of the various transport processes and chemical reactions occurring in a glass furnace is an enormous task. The overall problem involves characterization of the radiant heat transfer from the flame-fired refractory-lined gas volume above the surface of the melt. These transfer rates are intimately coupled with convective rates within the melt, the magnitudes of which are determined by the interaction of radiant transfer, conductive transfer, and, in the area of the port feed, by melting, chemical reaction, and gas generation and disengagement. Therefore, it is not surprising that the design of these furnaces has developed as an art. Uncertainties in the relation between thru-put rate (quantity of product glass withdrawn per unit time), heating rates, geometry, etc., presently make optimum furnace design an impossibility. However, the buoyancy-driven currents within the melt homogenize the glass and the modification of these currents can exert a profound influence on product quality and thru-put rate.

A third problem area involving buoyancy-driven contained flows deals with the containment of nuclear reactors such as the liquid metal fast breeder reactor. A spherical reactor core surrounded by a liquid in a spherical annulus is a typical configuration. The hot inner and cool outer surfaces are maintained at constant temperature and heat is transferred across the annulus primarily by means of buoyancy-driven natural convection flow. For practical values of the Rayleigh number, there is no theoretical method for calculating the heat transfer rate across the annulus and the scaling laws remain empirical.

A fourth area in which buoyancy-driven flows have become of interest is in the study of global plate tectonics and the theory of continental drift. While the existence of continental drift is almost universally accepted, the forces which cause the drift are not well understood. The upwelling of material from the Earth's interior near mid-ocean ridges and the return of material in subduction zones have led present-day investigators to suspect thermal convection currents as a possible motive force. The typical analysis considers steady natural convection between two horizontal infinite slabs heated from below and thus the geophysical problem is modeled by a geometry for which the horizontal length scale cannot be determined. While these calculations do indicate the possibility of geophysical flows being driven by buoyancy, they cannot be directly applicable to the continental drift problem because of the approximate spherical geometry of the Earth and the attendant global mass conservation restriction implied by a finite flow region. There is seismic evidence to support the theory that the Earth can be modeled as a solid spherical core and a thin spherical crust divided by

a molten annular region. The implications of such a model with regard to possible convection currents and associated internal shear layers have not been explored. Furthermore, the steady state assumption may not be justified, as we shall see.

Finally, long-term space missions will require storage of cyrogens in orbit. Heating by solar radiation leads to cryogen stratification in much the same manner as with liquified natural gas. Pumping limitations are determined by the onset of cryogen cavitation which, in turn, depends critically upon the stratification.

While these examples do not exhaust the various contained buoyancy-driven flows of interest, they do illustrate the breadth of application and the importance attached to such flows.

Earlier Work

There have been many efforts to analyze various models of the contained buoyancy-driven flow problem. We shall restrict our attention to the practically important flow regime that corresponds to large values of the Grashof number (the ratio of buoyant forces to viscous forces) and we will exclude that class of problems that deals with the stability of buoyancy-driven flows that is typified by the heat-from-below Rayleigh instability. Also we will consider laminar flow exclusively.

Previous efforts to analyze this large Rayleigh number, heated-from-the-side natural convection problem have used either ad hoc boundary-layer methods or purely numerical solutions by means of finite difference approximations. Typical of the earlier boundary-layer approaches is that of Bailey and Fearn [2] who considered the transient stratification of a cylindrical tank with hemispherical ends due to sidewall heating.

All of the heat input to the tank is assumed to appear as sensible heat in the sidewall boundary layer which empties into a uniformly mixed hot upper layer in the core and remains there. Mixing between the hot layer and the lower cold liquid in the core is neglected. Comparison with experiment is poor and can be attributed to two of the assumptions. First, the hot upper layer is not uniformly mixed, but is instead stratified. Thus the mass flux into and out of the sidewall boundary layer depends upon the time-dependent core stratification and cannot be a priori calculated by means of results for free convection along a flat plate in a medium with constant bulk temperature. Second, the boundary layer formed on the bottom hemispherical end is completely ignored without justification.

More recently Matulevicius [3] has measured both temperature and velocity in an unsteady stratified fluid in a high aspect ratio rectangular enclosure (initially at uniform temperature) which is heated uniformly on the sides and insulated on the top and bottom. These experiments have shown that the sidewall heating results in thin boundary layers being formed along the vertical walls. The boundary layer discharges fluid into the core region along the entire (time-varying) length of the stratified region. The greatest amount of fluid discharge occurs approximately at the interface of the stratified and unstratified regions in agreement with the experimental results of Schwind and Vliet [4]. Horizontal temperature gradients in the core are small. The warmer fluid deposited in the core settles downward like a "plug flow" as cooler fluid from the lower regions is fed into the sidewall boundary layer. Except for the top part of the core and a small region near the bottom, the axial temperature profile is linear after an initial transient period. Lastly,

an unexplained instability in the flow behavior was noted. Initially the flow appeared to be symmetrical about the central plane. However, in time the streamlines become skewed and the symmetry was destroyed. Similar results were observed in dye studies by Drake [5]. The temperature field was not appreciably affected by this instability.

Using these results, Matulevicius developed a thermal stratification model in which the flow is divided into two regions, a boundary layer rising at the heated wall and a central core. The boundary layer is assumed to be quasi-steady and the governing equations were solved by means of an integral method and the Prandtl number was assumed to be much greater than unity. By invoking the experimental result that the core temperature varies only vertically and assuming plug flow, Matulevicius calculated the core flow numerically using finite difference approximations. Comparison of these results with experiment was good.

While Matulevicius' work represents an important contribution because of the data obtained and the importance attached to the core-boundary layer interaction in the calculations, there are several limitations. The analysis is restricted to a rectangular geometry and a uniform heat flux at the sidewalls and is strictly applicable only when the Prandtl number is large. Further, details of the initial transients were obscured and certain simplifications in the core were not realized. Lastly, the results are obtained numerically and appropriate scaling laws are not wholly evident.

Integral methods have also been used by Emery and Chu [6] to calculate the steady state heat transfer rate across a rectangular enclosure with the top and bottom insulated and the two sides at different

constant temperatures. Comparison of the calculated heat-transfer rates with experiment is good although detailed flow properties are not available. The extension to the general problem is not considered.

Gill [7] has employed asymptotic methods to study the same steady flow near the horizontal centerline. Results obtained for the limiting case of infinite Prandtl number are in agreement with the experimental data of Elder [8]. The analysis does not apply to the flow away from the centerline and thus cannot be used to compute the total heat-transfer rate or describe the general flow pattern.

In a recent important contribution, Krane [9] has used similar methods to calculate the high Grashof number flow in the entire cavity. His calculations show that the flow divides itself into an inviscid stratified core (in which there is a pressure-buoyancy force balance) with nonlinear, nonsimilar free convection velocity and thermal boundary layers on the vertical walls and linear thermal boundary layers on the horizontal walls. The results stress the intimate coupling of the core flow and vertical wall boundary layers by means of entrainment and extrainment. That is, the core velocity field is given directly by the entrainment into (or extrainment from) the vertical wall boundary layer, the structure of which, in turn, depends upon the core. Comparison of the calculated total heat transfer rate with experiment is good.

Steady state calculations such as these are of interest (for a particular problem) in that they indicate the nature of the final asymptotic state. However, they are unable to analyze the important transient part of the problem. Also, existing calculations are generally restricted to rectangular cavities. Further, the nonlinear nature of the vertical

wall boundary layer rules out stability calculations which could provide a theoretical explanation for the occurrence of multicellular flows in high aspect ratio cavities undergoing sidewall heating.

Sakurai and Matsuda [10] consider a Boussinesq fluid at rest in a circular cylinder with its axis of symmetry parallel to the gravitational force. They analyze the unsteady flow that results from abruptly changing the sidewall temperature from its original profile, which is invariant around the cylinder (in a horizontal plane) and linear along the cylinder (in a vertical plane), to some new profile that is also linear along the cylinder. This new profile has a slightly greater rate-of-change than the original profile and is oriented such that the container is heated above its horizontal mid-plane and cooled below its mid-plane. They apply the linearized theory for the case where the Prandtl number is of order unity to find the temperature and velocity within the core region. They demonstrate the existence of a meridional circulation that is pumped by a sidewall boundary layer. This meridional circulation redistributes the fluid temperature to bring about a new state of stratification. The time scale for this temperature adjustment process is determined. This work by Sakurai and Matsuda is important in that for the first time an analytical solution has been developed for the transient natural convection flow of a fluid in a cavity that makes clear the basic physical processes that occur. The limitation to their work is that it applies only to the circular cylinder geometry with the particular linear boundary condition that they considered. Thus, the general problem of linearized bouyant motion in a closed container remains to be solved.

The main thrust of the recent research effort in contained

buoyancy-driven flows has concentrated on development of numerical solutions by means of finite-difference approximations. Although applicable in principle to arbitrary configurations, the computations deal almost exclusively with rectangular cavities and steady-state flows. For reasons of computation efficiency and stability it has become popular to solve the unsteady conservation equations with the asymptotic steady state being the result of interest. Thus, in principle, the unsteady problem can be analyzed numerically and these numerical solutions do enjoy some degree of success in predicting total heat-transfer rates and detailed features of the flowfield. However, limitations on computer storage space have prevented the finite difference models from being applied to the practically important high Grashof number regime. This occurs because the boundary-layer thickness decreases with increasing Grashof number, which requires, in turn, an increase in the number of gridpoints needed to adequately resolve the features of the flow in the boundary layer. While the use of variable mesh size can partly alleviate this difficulty, one still cannot carry out calculations for all Grashof numbers of interest. Furthermore, as pointed out by Emmons [11], there exists a number of serious questions concerning the adequacy of the convergence criteria used by those employing finite difference techniques. In the absence of mathematically rigorous proofs of accuracy and convergence, most numerical solutions are assumed to have "converged" when they "look good" when compared with preconceived trends in the data. It should also be noted that numerical solutions are quite costly in terms of computer time and programming manhours and thus are not suited for most design purposes. Most importantly, numerical solutions by their very nature do not readily indicate parameter trends or lend an understanding

to the basic physical phenomena occurring in a given problem. The effects of geometry changes cannot be assessed and the disparate time and length scales which occur in the practically important high Grashof number regime are not well suited to numerical solutions. Thus, it is apparent that more analytical and semi-analytical work (such as that done by Sakurai and Matsuda and Krane) is needed if advances in understanding the unsteady, buoyancy-driven contained flow problem are to be made.

Method of Attack

Natural convection is a phrase that is used to describe fluid flow that is driven by a gravitational body force. This body force, more commonly called the buoyant force, results solely from a nonhomogeneous density field if we consider the gravitational field to be invariant. Thus, a fluid is said to be stably stratified if the density gradient produces a buoyant force that tends to restore a perturbed fluid particle to its original position. We will focus our attention on stably stratified laminar natural convection in a closed container that is heated from the side. Thus, we will avoid that class of problems that deals with fundamentally unstable natural convection.

In the study of natural convection problems, it is a frequent practice to simplify the basic equations by introducing certain approximations that are attributed to Boussinesq [12]. The Boussinesq approximations are examined by Spiegel and Veronis [13], and they summarized them in two statements: (1) The fluctuations in density which appear with the advent of motion result principally from thermal (as opposed to pressure) effects. (2) In the equations for the rate-of-change of

momentum and mass, density variations may be neglected except when they are coupled to the gravitational acceleration in the buoyancy force. We shall develop the linearized equivalent of the "Boussinesq" equations in a rational manner and explicitly describe the approximations involved.

In the particular problem we will treat, we will consider an arbitrarily shaped closed container enclosing a Boussinesq fluid which is initially in some physically permissible stable state of rest. At an initial instant the temperature of the container will be impulsively changed. We will describe the ensuing unsteady laminar flow as well as the final asymptotic steady state that is governed by the linearized equations. We refer to this problem as the general heat-up problem since no restriction has been made as to the container geometry or container temperature profile. In requiring the initial state of rest to be stable, we are specifically excluding that class of problems dealing with the stability of buoyancy-driven flows typified by the heated-from-below Rayleigh instability. Many flows of practical interest correspond to large values of the Grashof number. We shall restrict our attention to this practically important flow regime. We shall also limit the Prandtl number to be of order unity. The solution to this general heat-up problem encompasses most linearized contained buoyant motions as special cases, and as such, should be of far-reaching practical interest.

Those who study stratified fluids are aware that a very close analogy exists between stratified fluid phenomena and rotating fluid phenomena. For example, Veronis [14] gives an extensive review of the analogy between rotating and stratified fluids and Greenspan [15] often mentions the analogy in his book on rotating fluid theory. A "rotating"

fluid is a fluid in which motion is capable of being driven by a Coriolis force. This Coriolis force plays the role of the buoyant force in the analogy with stratified fluids. Thus, both of these subjects have richly endowed structures for precisely the same reason -- they both support internal wave motion.

The analogy is derived from the fact that the linearized equations governing a rotating fluid and the linearized equations governing a stratified fluid can, in each case, be written as a single sixth-order partial differential equation for pressure (with different parameters in each case). However, the boundary conditions for a fluid dynamics problem cannot, in general, be written in terms of the pressure alone. Thus, even though the governing equation is the same for both a linearized rotating fluid and a linearized stratified fluid, the boundary conditions are not the same in general and an explicit analogy between rotating and stratified fluids is prevented.

There are certain special cases for which the governing equations and the boundary conditions can be made identical and then the analogy is "perfect". That is, the solution to a rotating problem can be generated from the analogous stratified solution by simply renaming the appropriate parameters. For example, Trustrum [16] considers inviscid, incompressible fluids flowing past a small disturbance in an infinite fluid domain to achieve the perfect analogy. As a rule, the special cases that allow the perfect analogy are not too appealing physically. A notable exception is the treatment of linearized buoyant motion due to an impulsively heated infinite vertical plate by Doty and Jischke [17]. For Prandtl number equal to unity, this result is completely analogous to the

so-called Ekman layer in rotating fluid theory. The Ekman layer is the boundary layer that forms on an infinite rotating plate when its angular velocity is impulsively increased slightly from an initial state where the plate and its surrounding fluid are rotating as a rigid body.

While it is a rare instance when one can draw an exact parallel between the phenomena in rotating and stratified fluid flow, a wide variety of phenomena in one physical system can be analyzed and understood in terms of the behavior in the analogous system. The increased understanding provided by the different viewpoints is one justification for developing the analogy in some detail. For example, Sakurai and Matsuda [10] were motivated in their work on the heat-up of a circular cylinder by the work done by Greenspan and Howard [18] on the spin-down process in a rotating fluid. A second reason is that laboratory studies may be more easily pursued in one of the two systems and experimental information pertinent to the other may be obtained.

The rotating fluid problem that is similar to our general heat-up problem for stratified fluids is the general spin-down problem treated by Greenspan [19]. He considers an arbitrarily shaped closed container filled with an incompressible fluid that is originally rotating as a rigid body with constant angular velocity. At an initial instant a physically acceptable initial state of fluid motion is prescribed. Greenspan then analyzes the ensuing transient motion and describes the ultimate return to rigid-body rotation. We will adapt the solution procedure used by Greenspan to solve our general heat-up problem for a stratified fluid.

Briefly, Greenspan's solution procedure is as follows: Expansions in half powers of the Ekman number (the fourth root of the reciprical of

the Rayleigh number is the appropriate parameter for stratified fluids) are introduced into the governing equations and a problem sequence is resolved. The first of these problems is for the zeroth-order solution for the inviscid interior region. In the second problem, the internal motion is corrected for viscous effects to make the basic tangential velocity zero at the boundary. However, the boundary layers induce further interior motion by establishing a small normal mass flux and this sets up a third problem. Once the secondary interior motion is determined from this third problem, it too must be corrected at the boundary. However, our analysis will end with this secondary circulation although, in principle, the procedure can be carried to higher order. The goal of our work then, is to adapt this solution procedure to the general heat-up problem for a stratified fluid and achieve an approximate solution for the motion that is uniformly valid in time and space.

CHAPTER II

THEORETICAL DEVELOPMENT

Governing Equations

Consider an arbitrarily shaped closed container, Σ, that is completely filled with a fluid that is initially in a stable state of rest. At an initial instant, $t = 0$, the temperature of Σ is impulsively changed. A description of the unsteady flow that ensues is desired.

Assume that the fluid is Newtonian and that it obeys Fourier's conduction law. Furthermore, assume that the first and second coefficients of viscosity, μ and λ, and the thermal conductivity, k, are constant. Also assume that the only body force acting on the fluid is a gravity force that acts in the negative z-direction with a constant magnitude of g per unit mass. With these assumptions, the equations that govern the fluid are

<u>mass</u>
$$\frac{D\rho}{Dt} + \rho \nabla \cdot \vec{V} = 0 \tag{2.1}$$

<u>momentum</u>
$$\rho \frac{D\vec{V}}{Dt} = - \nabla p + \mu \nabla^2 \vec{V} + (\mu+\lambda) \nabla (\nabla \cdot \vec{V}) - \rho g \hat{e}_z \tag{2.2}$$

<u>energy</u>
$$\rho c_p \frac{DT}{Dt} = \frac{\beta T}{\kappa} \left(\beta \frac{DT}{Dt} - \nabla \cdot \vec{V} \right) + \overleftrightarrow{\tau} : \overleftrightarrow{\varepsilon} + k \nabla^2 T \quad . \tag{2.3}$$

Here pressure, density, and temperature are given by p, ρ, and T, respectively. Velocity and time are $\vec{V}$ and t, respectively. The viscous stress tensor, $\overleftrightarrow{\tau}$, is related to the rate-of-strain tensor, $\overleftrightarrow{\varepsilon}$, according

to the Newtonian law

$$\overleftrightarrow{\tau} = 2\mu\overleftrightarrow{\epsilon} + \lambda(\nabla\cdot\vec{V})\overleftrightarrow{\Pi} \tag{2.4}$$

$$\overleftrightarrow{\epsilon} = \tfrac{1}{2}[\nabla\vec{V} + (\nabla\vec{V})^{+}] \quad . \tag{2.5}$$

The coefficient of thermal expansion and the coefficient of isothermal compression are given by β and $\varkappa$, respectively, where these coefficients are defined as

$$\beta \equiv -\frac{1}{\rho}\left(\frac{\partial\rho}{\partial T}\right)_p \tag{2.6}$$

$$\varkappa \equiv \frac{1}{\rho}\left(\frac{\partial\rho}{\partial p}\right)_T \quad . \tag{2.7}$$

This system of equations becomes closed upon the addition of the thermal equation of state

$$p = p(\rho, T) \tag{2.8}$$

and appropriate initial and boundary conditions.

Static Basic State

Assume that the fluid motion to be studied is a perturbation on a basic state of stable static equilibrium. Then the governing equations for this basic state (denoted by the subscript B) reduce to

$$\underline{\text{mom}} \quad \frac{dp_B}{dz} = -\rho_B g \tag{2.9}$$

$$\underline{\text{energy}} \quad \frac{d^2T_B}{dz^2} = 0 \tag{2.10}$$

$$\underline{\text{state}} \quad \frac{d\rho_B}{dz} = -\rho_B\left(\beta_B\frac{dT_B}{dz} - \varkappa_B\frac{dp_B}{dz}\right) \quad . \tag{2.11}$$

Let $z = 0$ represent the bottom of the container where the static temperature is defined to be the "operating" temperature T_{op}. Let $z = L$ represent the top of the container where the static temperature is

defined to be $T_{op} + \Delta T$. We will require ΔT to be positive in order to ensure that the basic state is statically stable. The energy equation may then be integrated to yield the basic temperature profile

$$T_B = T_{op} + \Delta T(z/L) \quad . \tag{2.12}$$

This basic state and the container geometry are illustrated in Figure (2.1).

Weak Stratification

Define weak stratification as that state for which any static thermodynamic variable, Q, can be represented by

$$Q/Q_{REP} = 1 + \text{higher order terms} \tag{2.13}$$

where Q_{REP} is some representative value of Q within the region of interest and the higher order terms are much less than unity. For example, we see from the basic temperature profile, Eq. (2.12), that if the basic stratification is to be weak then

$$\Delta T/T_{op} << 1 \quad . \tag{2.14}$$

This allows us to write

$$\begin{aligned} T_B/T_{op} &= 1 + (\Delta T/T_{op})(z/L) \\ &= 1 + \text{higher order terms} \end{aligned} \tag{2.15}$$

within the region of interest $0 \leq z \leq L$.

Similarly, the basic equation of state, Eq. (2.11), may be integrated to yield

$$\rho_B/\rho_{op} = 1 - (\beta_{op}\Delta T - \rho_{op}\mu_{op}gL)(z/L) + \ldots \tag{2.16}$$

and we see that weak stratification requires two more conditions

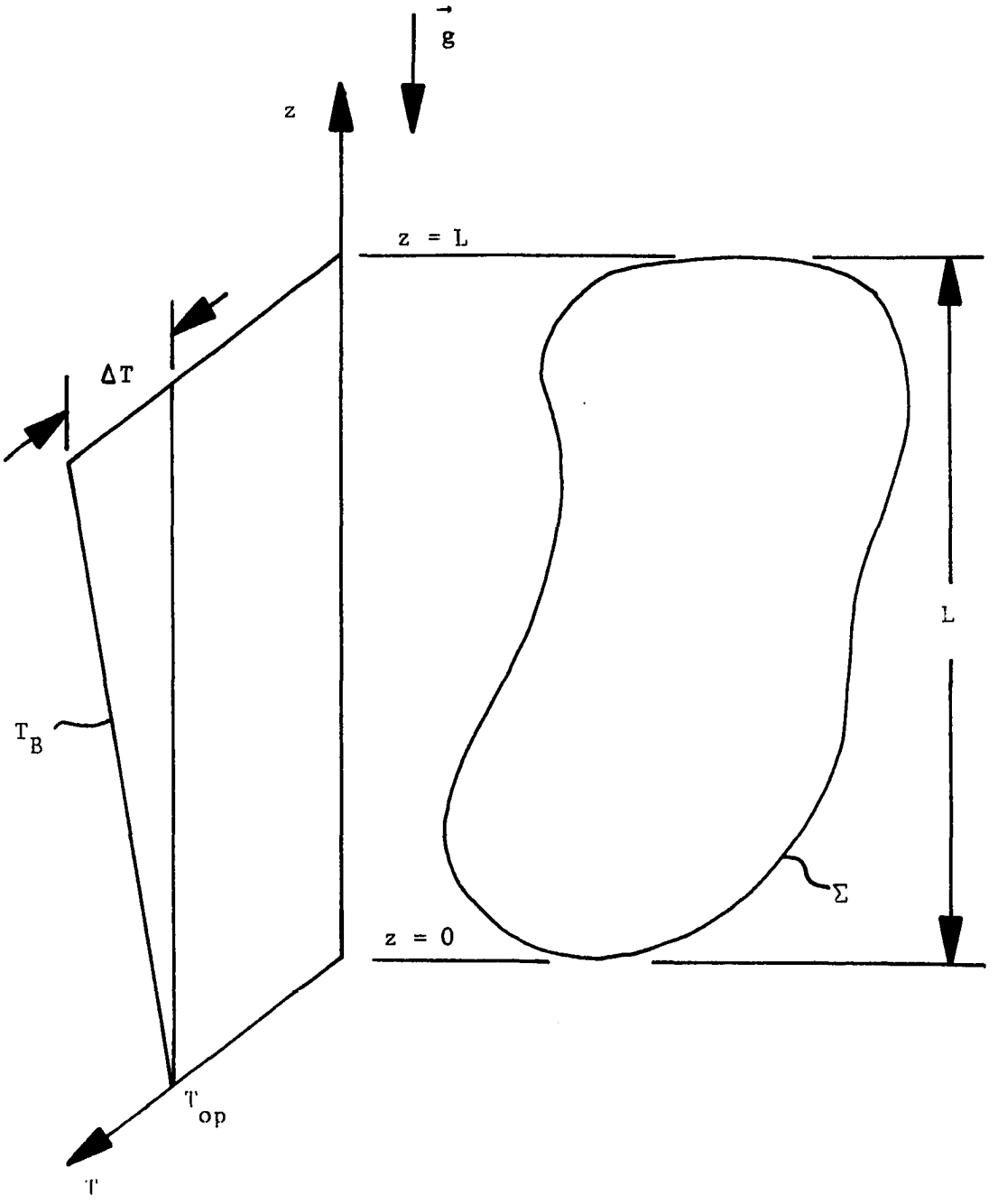

Figure 2.1 The Basic State and Container Geometry

$$\beta_{op}\Delta T << 1 \tag{2.17}$$

$$\rho_{op}\varkappa_{op}gL << 1 \quad . \tag{2.18}$$

The basic momentum equation, (2.9), may be integrated to yield

$$p_B/p_{op} = 1 - (\rho_{op}gL/p_{op})(z/L) + \ldots \tag{2.19}$$

which gives the fourth and final condition necessary for a weakly-stratified basic state to be

$$\rho_{op}gL/p_{op} << 1 \quad . \tag{2.20}$$

When the fluid being considered is a perfect gas, the coefficients of expansion and compression are given by $\beta = 1/T$ and $\varkappa = 1/p$. In this case, the four requirements for weak stratification reduce to two requirements which can be taken as $\Delta T/T_{op} << 1$ and $\rho_{op}gL/p_{op} << 1$. In words, the requirements for weak stratification of a perfect gas are:

(1) the vertical temperature change in the region of interest must be much less than the operating temperature of the region

(2) the static pressure due to the fluid within the region of interest must be much less than the operating pressure.

The requirements for weak stratification are met in many engineering problems. For example, air at STP in a 100 ft. container with $\Delta T = 10^{o}F$ yields $\Delta T/T_{op} \approx 0.02$ and $\rho_{op}g\ L/p_{op} \approx 0.004$.

Some fluids may deviate significantly from perfect gas behavior such that in addition to the two weak stratification conditions given in words above the other two conditions must also be checked in order to ensure that the fluid is weakly-stratified.

Nondimensional Equations

We may write each thermodynamic variable as the sum of its unperturbed basic value and a nondimensional perturbation (denoted by an asterisk) as follows:

$$p = p_B + p_{ref} p^* \qquad \beta = \beta_B + \beta_{ref} \beta^* \qquad (2.21\ a,b)$$

$$\rho = \rho_B + \rho_{ref} \rho^* \qquad \varkappa = \varkappa_B + \varkappa_{ref} \varkappa^* \qquad (2.22\ a,b)$$

$$T = T_B + T_{ref} T^* \qquad c_p = c_{p_B} + c_{p_{ref}} c_p^* \ . \qquad (2.23\ a,b)$$

Here the perturbation has been nondimensionalized by an, as yet, unspecified reference value. We also nondimensionalize velocity, time, and space by reference values in a similar way

$$\vec{V} = V_{ref} \vec{V}^* \qquad (2.24)$$

$$t = t_{ref} t^* \qquad (2.25)$$

$$\nabla = \nabla^* / L_{ref} \ . \qquad (2.26)$$

We may now substitute these expression into the governing equations, nondimensionalize each thermodynamic variable by its operating value, and obtain a set of nondimensional conservation equations. For example, this process for the continuity equation, starting with Eq. (2.1), is as follows:

mass $$\frac{D\rho}{Dt} + \rho \nabla \cdot \vec{V} = 0 \qquad (2.1)$$

$$\frac{\partial \rho}{\partial t} + \nabla \cdot \rho \vec{V} = 0 \qquad (2.27)$$

$$\frac{1}{t_{ref}} \frac{\partial}{\partial t^*} (\rho_B + \rho_{ref} \rho^*) + \frac{\nabla^*}{L_{ref}} \cdot (\rho_B + \rho_{ref} \rho^*) V_{ref} \vec{V}^* = 0 \qquad (2.28)$$

$$\frac{\rho_{ref}}{t_{ref}} \frac{\partial \rho^*}{\partial t^*} + \frac{V_{ref}}{L_{ref}} (\nabla^* \cdot \rho_B \vec{V}^* + \rho_{ref} \nabla^* \cdot \rho^* \vec{V}^*) = 0 \qquad (2.29)$$

$$\left(\frac{\rho_{ref}}{\rho_{op}}\frac{L_{ref}}{t_{ref}}\frac{1}{V_{ref}}\right)\frac{\partial\rho^*}{\partial t^*}+\nabla^*\cdot\left(\frac{\rho_B}{\rho_{op}}\vec{V}^*\right)+\left(\frac{\rho_{ref}}{\rho_{op}}\right)\nabla^*\cdot\rho^*\vec{V}^*=0\quad . \tag{2.30}$$

In a similar way, the momentum and energy equations may be written as

momentum

$$\left(\frac{\rho_B}{\rho_{op}}+\frac{\rho_{ref}}{\rho_{op}}\rho^*\right)\left(\frac{\partial\vec{V}^*}{\partial t^*}+\frac{t_{ref}}{L_{ref}}V_{ref}\vec{V}^*\cdot\nabla^*\vec{V}^*\right)=-\left(\frac{p_{ref}}{\rho_{op}}\frac{t_{ref}}{L_{ref}}\frac{1}{V_{ref}}\right)\nabla^*p^*$$

$$+\left(\frac{\mu}{\rho_{op}L_{ref}}\frac{t_{ref}}{L_{ref}}\right)\left[\nabla^{*2}\vec{V}^*+\left(1+\frac{\lambda}{\mu}\right)\nabla^*(\nabla^*\cdot\vec{V}^*)\right]$$

$$-\left(g\frac{\rho_{ref}}{\rho_{op}}\frac{t_{ref}}{V_{ref}}\right)\rho^*\hat{e}_z \tag{2.31}$$

energy

$$\left(\frac{\rho_B}{\rho_{op}}+\frac{\rho_{ref}}{\rho_{op}}\rho^*\right)\left(\frac{c_{p_B}}{c_{p_{op}}}+\frac{c_{p_{ref}}}{c_{p_{op}}}c_p^*\right)\left[\frac{\partial T^*}{\partial t^*}+\left(\frac{t_{ref}}{L_{ref}}V_{ref}\right)\left(\frac{\Delta T}{T_{ref}}\frac{L_{ref}}{L}W^*+\vec{V}^*\cdot\nabla^*T^*\right)\right]$$

$$=\left(\frac{\beta_{op}^2T_{op}}{\rho_{op}\mu_{op}c_{p_{op}}}\right)\frac{\left(\frac{\beta_B}{\beta_{op}}+\frac{\beta_{ref}}{\beta_{op}}\beta^*\right)\left(\frac{T_B}{T_{op}}+\frac{T_{ref}}{T_{op}}T^*\right)}{\left(\frac{\mu_B}{\mu_{op}}+\frac{\mu_{ref}}{\mu_{op}}\mu^*\right)}$$

$$\times\left[\left(\frac{\beta_B}{\beta_{op}}+\frac{\beta_{ref}}{\beta_{op}}\beta^*\right)\left(\frac{\partial T^*}{\partial t^*}+\left(\frac{t_{ref}}{L_{ref}}V_{ref}\right)\left(\frac{\Delta T}{T_{ref}}\frac{L_{ref}}{L}W^*+\vec{V}^*\cdot\nabla^*T^*\right)\right)\right.$$

$$\left.-\left(\frac{t_{ref}}{L_{ref}}\frac{V_{ref}}{T_{ref}}\frac{1}{\beta_{op}}\right)\nabla^*\cdot\vec{V}^*\right]+\left(\frac{\mu}{\rho_{op}c_{p_{op}}L_{ref}}\frac{t_{ref}}{L_{ref}}\frac{V_{ref}^2}{T_{ref}}\right)\overleftrightarrow{\tau}^*:\overleftrightarrow{e}^*$$

$$+\left(\frac{k}{\rho_{op}c_{p_{op}}L_{ref}}\frac{t_{ref}}{L_{ref}}\right)\nabla^{*2}T^*\quad . \tag{2.32}$$

Small Disturbances

If we define small disturbances to the basic state to be those perturbations for which $p_{ref}\,p^* << p_B$, $\rho_{ref}\,\rho^* << \rho_B$ and $T_{ref}T^* << T_B$;

then the assumption that p^*, ρ^* and T^* are of order unity leads to the conclusion that

$$p_{ref}/p_B \ , \ \rho_{ref}/\rho_B, \ T_{ref}/T_B << 1 \tag{2.33}$$

for a small-disturbance flow. In other words, the maximum flow-induced change to each thermodynamic variable is much less than its static value.

As a consequence of a small-disturbance assumption, the equation of state may be expanded in a Taylor series about the basic state as follows:

$$\begin{aligned}\rho(p,T) &= \rho(p_B + p_{ref}p^*, \ T_B + T_{ref}T^*) \\ &= \rho(p_B,T_B) + \left[\left(\frac{\partial\rho}{\partial p}\right)_T\right]_{p_B,T_B} p_{ref}p^* + \left[\left(\frac{\partial\rho}{\partial T}\right)_p\right]_{p_B,T_B} T_{ref}T^* + \ldots \\ &= \rho_B + \rho_B \varkappa_B \, p_{ref}p^* - \rho_B \beta_B \, T_{ref}T^* + \ldots \end{aligned} \tag{2.34}$$

Thus, by definition, we may write

$$\begin{aligned}\rho_{ref} \, \rho^* &\equiv \rho - \rho_B \\ &= -\rho_B(\beta_B \, T_{ref}T^* - \varkappa_B p_{ref}p^*) + \ldots \end{aligned} \tag{2.35}$$

This is the appropriate small-disturbance form of the equation of state.

Notice that if a small disturbance occurs in a weakly-stratified basic state then the equation of state may be further simplified as

$$\rho^* = -\left(\rho_{op}\beta_{op}\frac{T_{ref}}{\rho_{ref}}\right) T^* + \left(\rho_{op}\varkappa_{op}\frac{p_{ref}}{\rho_{ref}}\right) p^* + \ldots \tag{2.36}$$

Linearized Equations

We have been considering the problem of a fluid that is confined to an arbitrary closed container which is characterized by a vertical height L. Let us now assume that the fluid is initially in a weakly-stratified state of static equilibrium and that at an initial instant

the temperature of the container is changed by a "small" amount such that a small-disturbance flow results. Let this "small" temperature disturbance be characterized by $\epsilon\Delta T$ where ϵ is no more than order unity.

Now make the following assumptions:

(1) Assume that the temperature perturbation in the fluid will eventually be of the same order as that on the boundary. This implies $T_{ref} = \epsilon\Delta T$ if T* is to be of order unity.

(2) Assume that order unity temperature changes cause order unity density changes. Then the appropriate equation of state, Eq. (2.36), implies $\rho_{ref} = \epsilon\, \rho_{op}\beta_{op}\Delta T$.

(3) Assume that an order unity acceleration results from an order unity buoyant force. The momentum equation, Eq. (2.31), then requires $V_{ref}/t_{ref} = \epsilon g\beta_{op}\Delta T$.

(4) Assume that the appropriate length scale is the characteristic height of the container so that $L_{ref} = L$.

(5) Assume that the pressure force and the buoyant force balance in the steady inviscid interior region (anticipating boundary-layer behavior) to obtain $p_{ref} = \epsilon\, \rho_{op} gL\beta_{op}\Delta T$ from Eq. (2.31).

(6) Assume that the unsteady energy term and the lowest-order convected energy term balance to derive $t_{ref}V_{ref} = \epsilon L$ from Eq. (2.32).

In summary, the reference values are

$$p_{ref}/p_{op} = \epsilon\,(\rho_{op} gL/p_{op})(\beta_{op}\Delta T) \tag{2.37}$$

$$\rho_{ref}/\rho_{op} = \epsilon\,(\beta_{op}\Delta T) \tag{2.38}$$

$$T_{ref}/T_{op} = \epsilon\,(\Delta T/T_{op}) \tag{2.39}$$

$$V_{ref} = \epsilon\, LN \tag{2.40}$$

$$t_{ref} = 1/N \tag{2.41}$$

$$L_{ref} = L \tag{2.42}$$

where

$$N \equiv \sqrt{\frac{g}{L}\beta_{op}\Delta T} \tag{2.43}$$

is the so-called "Brunt-Väisälä" frequency.

Two important observations can be made by inspecting these reference values. First, notice that an order unity time corresponds to the period of a simple pendulum of reference length that is oscillating in a "stratified-reduced" gravity field, $g\beta_{op}\Delta T$. Second, notice that the weak-stratification assumption and the small-disturbance assumption are compatible for ϵ up to order unity. For example, we see from Eq. (2.39) that if $\Delta T/T_{op}$ is much less than unity (weak stratification) then T_{ref}/T_{op} is also much less than unity (small disturbance) as long as ϵ is no more than order unity. As a consequence, we will see that the weak-stratification assumption and the small-disturbance assumption, as we have defined them here, are not sufficient to produce a linear set of equations.

Before substituting the reference values back into the governing equations, let us define the following parameters:

$$G_r \equiv \rho_{op}^2 g L^3 \beta_{op} \Delta T/\mu^2 = \text{Grashof number} \tag{2.44}$$

$$P_r \equiv \mu c_{p_{op}}/k = \text{Prandtl number} \tag{2.45}$$

$$M \equiv \beta_{op} T_{op} gL/(c_{p_{op}} \Delta T) = \text{Compressibility factor} \tag{2.46}$$

Then the equations governing weakly-stratified, small-disturbance flow become

$$\underline{\text{mass}} \quad \beta_{op}\Delta T \frac{\partial \rho^*}{\partial t^*} + \nabla^* \cdot \frac{\rho_B}{\rho_{op}} \vec{V}^* + \epsilon \beta_{op} \Delta T \nabla^* \cdot \rho^* \vec{V}^* = 0 \tag{2.47}$$

momentum

$$\left(\frac{\rho_B}{\rho_{op}} + \epsilon\ \beta_{op}\Delta T\ \rho^*\right)\left(\frac{\partial \vec{V}^*}{\partial t^*} + \epsilon\ \vec{V}^*\cdot\nabla^*\vec{V}^*\right) = -\nabla^* p^*$$

$$+ G_r^{-\frac{1}{2}}\left[\nabla^{*2}\vec{V}^* + \left(1 + \frac{\lambda}{\mu}\right)\nabla^*(\nabla^*\cdot\vec{V}^*)\right] - \rho^*\,\hat{e}_z \qquad (2.48)$$

energy

$$\left(\frac{\rho_B}{\rho_{op}} + \epsilon\ \beta_{op}\Delta T\ \rho^*\right)\left(\frac{c_{p_B}}{c_{p_{op}}} + \frac{c_{p_{ref}}}{c_{p_{op}}}\ c_p^*\right)\left(\frac{\partial T^*}{\partial t^*} + W^* + \epsilon\ \vec{V}^*\cdot\nabla^*T^*\right)$$

$$= \frac{\beta_{op}^2\ T_{op}}{\rho_{op}\nu_{op}c_{p_{op}}}\ \frac{\left(\frac{\beta_B}{\beta_{op}} + \frac{\beta_{ref}}{\beta_{op}}\beta^*\right)\left(\frac{T_B}{T_{op}} + \frac{\epsilon\Delta T}{T_{op}}\ T^*\right)}{\left(\frac{\nu_B}{\nu_{op}} + \frac{\nu_{ref}}{\nu_{op}}\ \nu^*\right)}$$

$$\times\left[\left(\frac{\beta_B}{\beta_{op}} + \frac{\beta_{ref}}{\beta_{op}}\beta^*\right)\left(\frac{\partial T^*}{\partial t^*} + W^* + \epsilon\ \vec{V}^*\cdot\nabla^*T^*\right) - \frac{1}{\beta_{op}\Delta T}\nabla^*\cdot\vec{V}^*\right]$$

$$+ \frac{G_r^{-\frac{1}{2}}}{P_r}\left[\epsilon\ M\ \frac{\Delta T}{T_{op}}\ P_r\ \overleftrightarrow{\tau}^*:\overleftrightarrow{\epsilon}^* + \nabla^{*2}T^*\right] \qquad (2.49)$$

state

$$\rho^* = -\ T^* + \rho_{op}\nu_{op}gLp^* \quad . \qquad (2.50)$$

The compressibility factor, M, is generally very small. For example, air at STP with L = 100 ft yields $M\ \Delta T/T_{op} \approx 0.001$. Thus, the viscous dissipation term in the energy equation can be neglected in comparison with the conduction term for most values of the Prandtl number. However, notice that very large Prandtl number flows are inherently nonlinear due to viscous dissipation.

We assume that

$$\beta_{op}\Delta T,\ \rho_{op}\nu_{op}gL,\ M << 1 \qquad (2.51)$$

and

$$P_r << \frac{T_{op}}{\epsilon\ M\ \Delta T}\ . \qquad (2.52)$$

Then, to lowest order, the equations governing weakly-stratified, small-disturbance flow become

<u>mass</u> $$\nabla^* \cdot \vec{V}^* = 0 \tag{2.53}$$

<u>momentum</u> $$\frac{\partial \vec{V}^*}{\partial t^*} + \epsilon\, \vec{V}^* \cdot \nabla^* \vec{V}^* = - \nabla^* p^* + G_r^{-\frac{1}{2}} \nabla^{*2} \vec{V}^* - \rho^* \hat{e}_z \tag{2.54}$$

<u>energy</u> $$\frac{\partial T^*}{\partial t^*} + W^* + \epsilon\, \vec{V}^* \cdot \nabla^* T^* = \frac{G_r^{-\frac{1}{2}}}{P_r} \nabla^{*2} T^* \tag{2.55}$$

<u>state</u> $$\rho^* = - T^* \tag{2.56}$$

The order of the terms neglected in these equations is $\beta_{op} \Delta T$ and $\rho_{op} \nu_{op} g L$.

These equations are valid for ϵ up to order unity. Thus, a linear set of equations is obtained if we further restrict ϵ to be much less than unity which corresponds to a "very small" change in the boundary temperature as depicted in Figure (2.2).

It is convenient to eliminate the Grashof number in favor of the Rayleigh number since this will yield steady state solutions that depend on only one parameter, the Rayleigh number, instead of the present two-parameter steady solutions that depend on the Grashof number and the Prandtl number.

Let $$R_a \equiv P_r G_r = \text{Rayleigh number} \tag{2.57}$$

and restrict the Prandtl number to be of order unity. Renormalize velocity and time as

$$\vec{V}^+ \equiv \sqrt{P_r}\, \vec{V}^* \tag{2.58}$$

$$t^+ \equiv \sqrt{P_r}\, t^* \tag{2.59}$$

and let the other variables remain unchanged. That is, let

$$p^+ \equiv p^* \tag{2.60}$$

NOTE:

(1) T_B is a weakly-stratified basic state since $\Delta T/T_{op} << 1$.

(2) T_Σ is a "very small" temperature perturbation since $\epsilon << 1$.

(3) $T^*_\Sigma = (T_\Sigma - T_B)/\epsilon \Delta T$ is a normalized temperature perturbation.

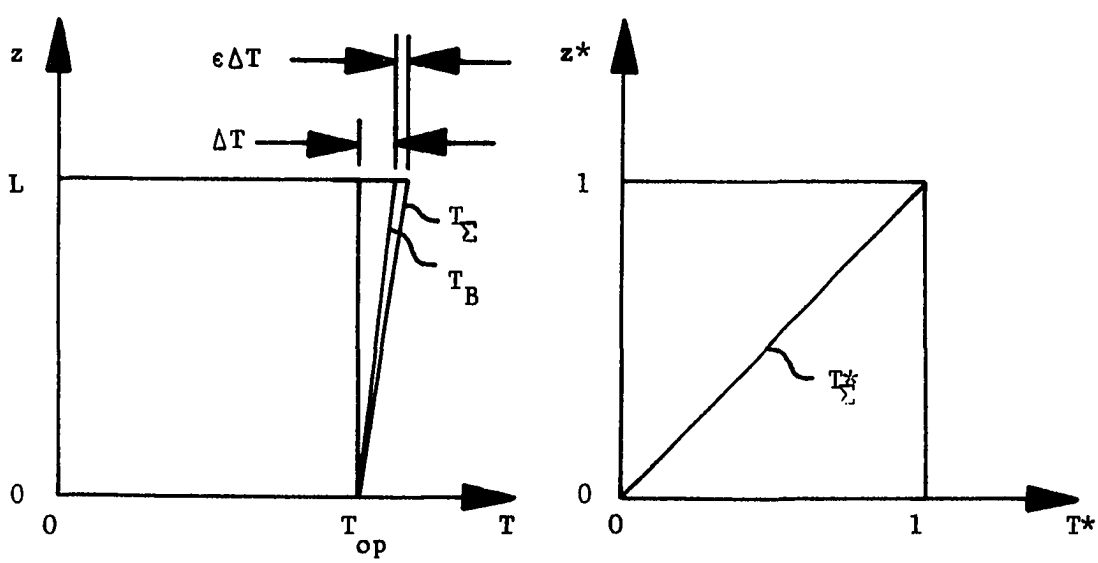

Figure 2.2 A Typical Temperature Perturbation Leading to Linearized Flow

$$\rho^+ \equiv \rho^* \tag{2.61}$$

$$T^+ \equiv T^* \quad . \tag{2.62}$$

Then the linear equations become

mass $$\nabla^+ \cdot \vec{V}^+ = 0$$

momentum $$\frac{\partial \vec{V}^+}{\partial t^+} = - \nabla^+ p^+ + R_a^{-\frac{1}{2}} \nabla^{+2} \vec{V}^+ - \rho^+ \hat{e}_z \tag{2.64}$$

energy $$P_r \frac{\partial T^+}{\partial t^+} + W^+ = R_a^{-\frac{1}{2}} \nabla^{+2} T^+ \tag{2.65}$$

state $$\rho^+ = - T^+ \quad . \tag{2.66}$$

This set of equations is equivalent to the so-called "Boussinesq" approximation that is often applied irrationally in the study of natural convection flows. However, the assumptions of a weakly-stratified basic state and very small disturbances allowed the rational development of these equations in this case.

It should be mentioned that the normalization used here depends on the fact that ΔT is not zero. In other words, even through the basic state is only weakly-stratified, that stratification is crucial and the case of zero stratification is fundamentally nonlinear.

Perturbation Expansion

The heat-up problem for an arbitrarily shaped closed container is governed by a set of linear partial differential equations when the basic state is a weakly-stratified state of rest and the change in the boundary temperature is very small. Dropping the superscript notation, we may write these equations as

$$\nabla \cdot \vec{V} = 0 \tag{2.67}$$

$$\frac{\partial \vec{V}}{\partial t} = - \nabla p + R_a^{-\frac{1}{2}} \nabla^2 \vec{V} + T \hat{e}_z \tag{2.68}$$

$$P_r \frac{\partial T}{\partial t} + W = R_a^{-\frac{1}{2}} \nabla^2 T \quad . \tag{2.69}$$

Here we have substituted the state equation into the momentum equation.

To complete the formulation of the problem, we add the following initial and boundary conditions:

$$\begin{cases} t = 0 : \vec{V}(\vec{r},0) = T(\vec{r},0) = 0 & \text{static equil. initially} \quad (2.70) \\ \text{on } \Sigma : T(\vec{r}_\Sigma,t) = H(t) T_\Sigma(\vec{r}_\Sigma) & \text{boundary temperature} \quad (2.71) \\ \text{on } \Sigma : \vec{V}(\vec{r}_\Sigma,t) = 0 & \text{no-slip on container} \quad (2.72) \\ t \to \infty : \vec{V},\ T \text{ finite} & \text{bounded solution} \quad (2.73) \end{cases}$$

where H(t) is the Heaviside step function, $T_\Sigma(\vec{r}_\Sigma)$ is the temperature profile on the boundary, and $\vec{r}_\Sigma$ is the position vector to some point on the container.

We will now make several assumptions based primarily on work done by Doty and Jischke [17] which gives an exact solution to the problem of linearized natural convection flow past an impulsively heated infinite vertical plate. We will assume that the Rayleigh number is large (a typical value for air at STP is 10^8 per L^3 where L is the container height in feet) and that viscous action and heat conduction are confined to thin boundary layers at the container walls throughout the principal phase of the motion (the boundary-layer dissipation time is anticipated to be of order $R_a^{\frac{1}{4}}$). These boundary layers produce a secondary motion that is of major importance by means of a "buoyancy-induced" transport of internal energy. Buoyancy, in this fashion, adjusts the temperature profile to its steady-state value in the "heat-up" time scale, $R_a^{\frac{1}{4}}$, and $R_a^{-\frac{1}{4}}$ emerges as the significant expansion parameter.

An approximate solution is sought that consists of an inviscid motion throughout the interior of the container that is matched to a motion in the viscous boundary layer in order to satisfy the boundary conditions. Furthermore, the representation must be uniformly valid in time and space to ensure that all the important phenomena are included and described. The solution procedure is to expand the flow variables in powers of $R_a^{-\frac{1}{4}}$, introduce these expansions into the governing equations, and resolve a problem sequence. The first of these problems is for the zeroth-order inviscid interior motion. In the second problem, the internal motion is corrected for viscous effects to make the velocity zero at the boundary. These boundary layers induce further interior motion by establishing a small mass flux normal to the boundary which requires a third problem to correct the interior motion. The analysis ends with this first-order correction to the interior motion, although in principle, higher order corrections could be carried out.

It is anticipated (again from reference [17]) that the pressure force and the buoyant force will be in balance over many periods of the Brunt-Väisälä frequency within the inviscid interior and that the interior will change slowly, without oscillation, from its initial value to its final value on the heat-up time scale. Thus, the assumed form of the interior solution is given by

$$\vec{V} = \vec{V}(\vec{r},\tau) \tag{2.74}$$

$$p = p(\vec{r},\tau) \tag{2.75}$$

$$T = T(\vec{r},\tau) \tag{2.76}$$

where

$$\tau = R_a^{-\frac{1}{4}} t \ . \tag{2.77}$$

This inviscid solution must be corrected for viscous action near the boundary, which in turn induces further inviscid motion in the

interior, etc. The boundary layers produced by the temperature perturbation become fully developed in a relatively short time (a few periods of the Brunt-Väisälä frequency) and then change very slowly during heat-up. Thus, as far as the inviscid motion is concerned, the boundary layers can be considered to be formed instantaneously and to remain steady throughout the heat-up process. As a consequence, the initial condition on the velocity must be given up. That is, the interior fluid will not be at rest initially, within the framework of this analysis, but will have some initial first-order motion that is dictated by the boundary-layer "suction".

Of course, we lose the capability of exactly describing the boundary layers and associated secondary flow at the very earliest time, but only then. Furthermore, these boundary layers and secondary flows are substantially the same as those determined from the earlier theory of Doty and Jischke [17] that treats the simpler flat plate geometry.

Based on these notions from the physics of the flow an approximate solution of the following form is sought:

$$\vec{V} = \vec{V}_0(\vec{r},\tau) + \tilde{\vec{V}}_0 + R_a^{-\frac{1}{4}}\left[\vec{V}_1(\vec{r},\tau) + \tilde{\vec{V}}_1\right] + \ldots \tag{2.78}$$

$$p = p_0(\vec{r},\tau) + \tilde{p}_0 + R_a^{-\frac{1}{4}}\left[p_1(\vec{r},\tau) + \tilde{p}_1\right] + \ldots \tag{2.79}$$

$$T = T_0(\vec{r},\tau) + \tilde{T}_0 + R_a^{-\frac{1}{4}}\left[T_1(\vec{r},\tau) + \tilde{T}_1\right] + \ldots \tag{2.80}$$

The tilde symbol denotes a boundary-layer function of a stretched boundary-layer coordinate, ξ. These functions approach zero exponentially fast as $\xi \to \infty$, which corresponds to the outer edge of the boundary layer. The functions without tildes are then the solution of the inviscid equations of motion. The replacement of the dependent variables by such a decomposition leads to a modified system of equations within

a singular perturbation scheme of analysis.

Let $\hat{n}$ be defined as the outward pointing unit normal to the container Σ. The fluid velocity in the boundary layer can then be resolved into components that are normal and tangential to Σ. This is expressed as

$$\tilde{\vec{V}} = (\tilde{\vec{V}} \cdot \hat{n})\hat{n} - (\tilde{\vec{V}} \times \hat{n}) \times \hat{n} \quad . \tag{2.81}$$

This expression can be substituted into the conservation equations and the tangential derivatives along Σ of any flow variable can be neglected when compared directly with normal derivatives of the same function to lead to the following set of equations which are valid in the boundary layer:

<u>mass</u>
$$\frac{\partial}{\partial \xi}(\tilde{\vec{V}} \cdot \hat{n}) + R_a^{-\frac{1}{2}} \hat{n} \cdot \nabla \times (\tilde{\vec{V}} \times \hat{n}) = 0 \tag{2.82}$$

<u>momentum</u>
$$\frac{\partial \tilde{p}}{\partial \xi} \hat{n} = R_a^{-\frac{1}{2}} \left[\frac{\partial \tilde{\vec{V}}}{\partial t} + \nabla_2 \tilde{p} - \frac{\partial^2 \tilde{\vec{V}}}{\partial \xi^2} - \tilde{T} \hat{e}_z \right] \tag{2.83}$$

<u>energy</u>
$$P_r \frac{\partial \tilde{T}}{\partial t} + \tilde{W} = \frac{\partial^2 \tilde{T}}{\partial \xi^2} \quad . \tag{2.84}$$

Here ∇_2 is defined as the two-dimensional gradient operator with components in the plane of Σ. The formal development of these equations can proceed in several equivalent ways and the presentation here is taken from Greenspan [15] who, in turn, based his work in part on that of Crabtree, Küchemann and Sowerby [20].

Problem Sequence

Substitution of the perturbation expansions into the governing equations and boundary conditions, Eqs. (2.67) through (2.73), leads to a sequence of problems for the inviscid interior flow, the boundary-layer flow and their mutual interactions. The problem sequence is as follows:

Problem A1: The Zeroth-Order Interior

$$\nabla \cdot \vec{V}_0 = 0 \tag{2.85}$$

$$\nabla p_0 = T_0 \, \hat{e}_z \tag{2.86}$$

$$W_0 = 0 \tag{2.87}$$

$$\text{with} \begin{cases} \vec{V}_0 \cdot \hat{n} = 0 \text{ on } \Sigma \end{cases} \tag{2.88}$$

Problem A2: The First-Order Boundary Layer

$$\frac{\partial}{\partial \xi} (\tilde{\vec{V}}_1 \cdot \hat{n}) = - \hat{n} \cdot \nabla \times (\tilde{\vec{V}}_0 \times \hat{n}) \tag{2.89}$$

$$- \frac{\partial \tilde{p}_1}{\partial \xi} \hat{n} = \frac{\partial^2 \tilde{\vec{V}}_0}{\partial \xi^2} + \tilde{T}_0 \, \hat{e}_z \tag{2.90}$$

$$\tilde{W}_0 = \frac{\partial^2 \tilde{T}_0}{\partial \xi^2} \tag{2.91}$$

$$\text{with} \begin{cases} \vec{V}_0 + \tilde{\vec{V}}_0 = 0 \text{ on } \Sigma & (2.92a) \\ \tilde{T}_0 + \tilde{T}_0 = T_\Sigma \text{ on } \Sigma & (2.92b) \end{cases}$$

Problem A3: The First-Order Interior

$$\nabla \cdot \vec{V}_1 = 0 \tag{2.93}$$

$$\frac{\partial \vec{V}_0}{\partial \tau} = - \nabla p_1 + T_1 \, \hat{e}_z \tag{2.94}$$

$$P_r \frac{\partial T_0}{\partial \tau} + W_1 = 0 \tag{2.95}$$

$$\text{with} \begin{cases} \vec{V}_1 + \tilde{\vec{V}}_1 = 0 \text{ on } \Sigma & (2.96) \\ T_0 = 0 \text{ at } \tau = 0 & (2.97) \end{cases}$$

The zeroth-order boundary-layer equations yield the trivial results

$$\tilde{\vec{V}}_0 \cdot \hat{n} = \tilde{p}_0 = 0 \tag{2.98}$$

which have been incorporated into the first-order problem. These results follow from the fact that the zeroth-order equations show that $\tilde{\vec{V}}_0 \cdot \hat{n}$ and $\tilde{p}_0$ are constants and these constants must be zero if the boundary layer is to decay to zero exponentially in ξ.

Finally, notice that the vorticity equation for the inviscid interior shows that the vertical component of vorticity is always zero to all orders of approximation. To see this, simply take the curl of the momentum equation, Eq. (2.68), to obtain the vorticity equation

$$\frac{\partial \vec{\omega}}{\partial t} = R_a^{-\frac{1}{2}} \nabla^2 \vec{\omega} + \nabla T \times \hat{e}_z \tag{2.99}$$

where $\vec{\omega} \equiv \text{curl } \vec{V}$. Then, if we neglect the viscous term, the vertical component of this equation is

$$\frac{\partial}{\partial t} (\hat{e}_z \cdot \vec{\omega}) = 0 \quad . \tag{2.100}$$

Thus, we see that the vertical component of vorticity is constant for all time and since the fluid starts from a state of rest that constant must be zero. Hence, the fluid will never contain any vertical vorticity in the inviscid interior. This is true before, during and after the initial instant in which the boundary layers form. This result is crucial to the analysis that follows.

CHAPTER III

ANALYSIS

Analysis of the general heat-up problem requires solving problems A1, A2 and A3 for the interior flow, the boundary-layer correction, and their mutual interaction. The solution to these problems will be taken up now.

Zeroth-Order Interior

Problem A1, which describes the zeroth-order interior flow, is

$$\underline{\text{mass}} \quad \nabla \cdot \vec{V}_o = 0 \tag{3.1}$$

$$\underline{\text{mom}} \quad \nabla p_o = T_o \hat{e}_z \tag{3.2}$$

$$\underline{\text{energy}} \quad W_o = 0 \tag{3.3}$$

$$\text{with} \quad \left\{ \vec{V}_o \cdot \hat{n} = 0 \text{ on } \Sigma \right. \quad . \tag{3.4}$$

The curl of the momentum equation yields $\nabla T_o x \hat{e}_z = 0$, which shows that T_o depends only on the vertical spatial coordinate z. Of course time enters into the description of the interior flow, but only as a parameter. Further analysis of the zeroth-order interior must be deferred until problem A3 is considered.

First-Order Boundary Layer

The first-order boundary layer is described by problem A2, which is given by

$$\underline{\text{mass}} \qquad \frac{\partial}{\partial \xi}\left(\tilde{\vec{V}}_1 \cdot \hat{n}\right) = -\,\hat{n} \cdot \nabla \times \left(\tilde{\vec{V}}_0 \times \hat{n}\right) \tag{3.5}$$

$$\underline{\text{mom}} \qquad -\frac{\partial \tilde{p}_1}{\partial \xi}\,\hat{n} = \frac{\partial^2 \tilde{\vec{V}}_0}{\partial \xi^2} + \tilde{T}_0\,\hat{e}_z \tag{3.6}$$

$$\underline{\text{energy}} \qquad \tilde{W}_0 = \frac{\partial^2 \tilde{T}_0}{\partial \xi^2} \tag{3.7}$$

$$\text{with} \qquad \begin{cases} \vec{V}_0 + \tilde{\vec{V}}_0 = 0 \text{ on } \Sigma & (3.8) \\ T_0 + \tilde{T}_0 = T_\Sigma \text{ on } \Sigma \quad . & (3.9) \end{cases}$$

The scalar components of the momentum equation normal to the container and in the vertical direction are

$$\underline{\hat{n}\cdot\text{mom}} \qquad -\frac{\partial \tilde{p}_1}{\partial \xi} = \tilde{T}_0 (\hat{n}\cdot\hat{e}_z) \tag{3.10}$$

$$\underline{\hat{e}_z\cdot\text{mom}} \qquad -\frac{\partial \tilde{p}_1}{\partial \xi}(\hat{n}\cdot\hat{e}_z) = \frac{\partial^2 \tilde{W}_0}{\partial \xi^2} + \tilde{T}_0 \tag{3.11}$$

where we have used the condition $\tilde{\vec{V}}_0 \cdot \hat{n} = 0$ from Eq. (2.98).

By combining these two scalar momentum equations with the energy equation, we derive a single fourth-order equation for the boundary-layer temperature which may be written as

$$\frac{\partial^4 \tilde{T}_0}{\partial \xi^4} + \left[1 - (\hat{n}\cdot\hat{e}_z)^2\right] \tilde{T}_0 = 0 \quad . \tag{3.12}$$

It is convenient to rescale the boundary-layer variable, ξ, as follows

$$\xi^* \equiv \sqrt[4]{\frac{1-(\hat{n}\cdot\hat{e}_z)^2}{4}}\;\xi \quad . \tag{3.13}$$

Then the equation for the boundary-layer temperature becomes simply

$$\frac{\partial^4 \tilde{T}_0}{\partial \xi^{*4}} + 4\,\tilde{T}_0 = 0 \quad . \tag{3.14}$$

Standard methods for solving ordinary differential equations may applied to this equation since all variables other than the boundary-layer

variable are parameters in this problem. Four functions of integration must be evaluated. The fact that $\tilde{T}_0$ must decay exponentially allows two of them to be set to zero. The third and fourth functions can be shown to be equal from the no-slip condition and thus the solution can be found in terms of a function of integration that must be determined by the specification of the temperature on the boundary. This solution is found to be

$$\tilde{T}_0 = \tilde{T}_0(\vec{r}_\Sigma;\tau)\ \exp(-\xi^*)\ \cos\ \xi^* \tag{3.15}$$

where $\vec{r}_\Sigma$ is the position vector to some point on the container and $\tilde{T}_0(\vec{r}_\Sigma;\tau)$ is the boundary-layer temperature on the container.

As we have already seen, the component of the zeroth-order boundary-layer velocity that is normal to the container wall must vanish and thus the entire zeroth-order boundary-layer velocity is tangent to the container. Hence, the vector momentum equation that describes the boundary-layer flow in a direction tangent to the container is

$$\frac{\partial^2 \tilde{\vec{V}}_0}{\partial \xi^2} = \tilde{T}_0\ (\hat{e}_z x \hat{n})\ x\ \hat{n}\ . \tag{3.16}$$

The expression just found for the temperature can be substituted into this equation. Then, by integrating twice, and using the fact that the boundary-layer velocity must decay exponentially across the boundary layer, we find the zeroth-order boundary-layer velocity to be

$$\tilde{\vec{V}}_0 = \tilde{T}_0(\vec{r}_\Sigma;\tau)\left[\frac{(\hat{n}x\hat{e}_z)\ x\ \hat{n}}{|\hat{n}\ x\ \hat{e}_z|}\right]\ \exp(-\xi^*)\sin\ \xi^*\ . \tag{3.17}$$

Let $\mathcal{C}_\ell$ be the curve that is formed by intersecting Σ with some horizontal "cross plane" such that $\mathcal{C}_\ell$ bounds the cross-plane area A as shown in Figure (3.1). Define $\hat{n}^*$ to be the normalized component of the

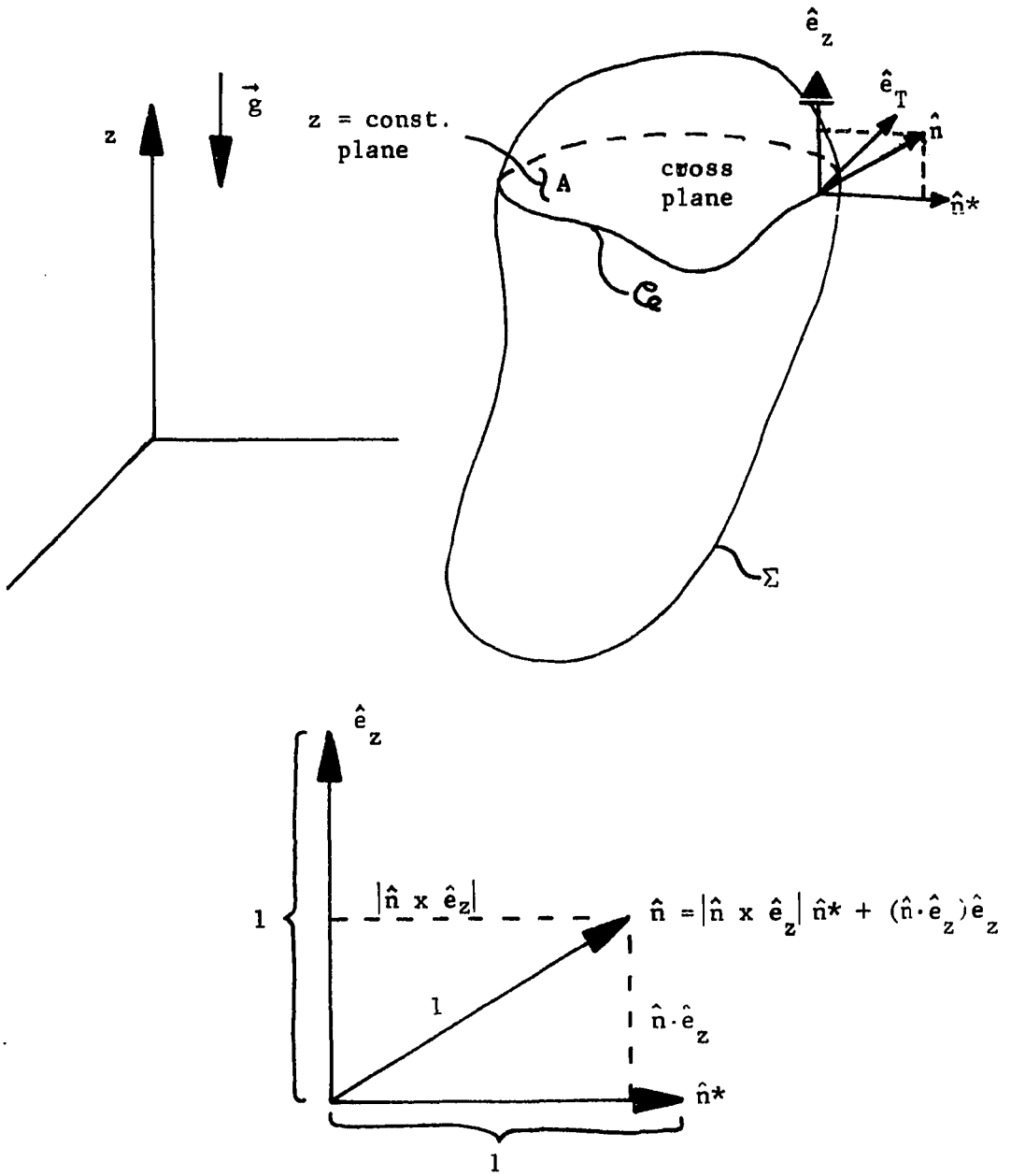

Figure 3.1 Cross-Plane Geometry and Unit Vectors

container's outward pointing unit normal, $\hat{n}$, such that $\hat{n}^*$ lies in the cross plane. Then $\hat{n}$ and $\hat{n}^*$ are related by

$$\hat{n} = |\hat{n} \times \hat{e}_z| \; \hat{n}^* + (\hat{n} \cdot \hat{e}_z)\hat{e}_z \tag{3.18}$$

as can be seen from the figure. Define $\hat{e}_T$ to be a unit vector that is tangent to $\mathcal{C}_Q$ in the cross plane. Then $\hat{e}_T$ is related to $\hat{n}$ by

$$\hat{e}_T = \frac{\hat{e}_z \times \hat{n}}{|\hat{e}_z \times \hat{n}|} \tag{3.19}$$

and $(\hat{n}^*, \hat{e}_T, \hat{e}_z)$ form an orthonormal triad on the container as also shown in Figure (3.1).

Thus, in terms of $\hat{e}_T$, we may rewrite Eq. (3.17) as

$$\tilde{\vec{V}}_0 = \tilde{T}_0(\vec{r}_\Sigma;\tau)(\hat{n} \times \hat{e}_T) \exp(-\xi^*)\sin \xi^* \quad . \tag{3.20}$$

Hence, we find that $\tilde{\vec{V}}_0 \times \hat{n}$ is given by

$$\tilde{\vec{V}}_0 \times \hat{n} = \tilde{T}_0(\vec{r}_\Sigma;\tau)\, \hat{e}_T \exp(-\xi^*)\sin \xi^* \quad . \tag{3.21}$$

Then the continuity equation, Eq. (3.5), may be integrated across the boundary layer to yield the first-order normal component of the boundary-layer velocity on the container. This boundary-layer "suction" is given by

$$(\tilde{\vec{V}}_1 \cdot \hat{n})_\Sigma = \frac{1}{\sqrt{2}} \; \hat{n} \cdot \nabla \times \left[\frac{\tilde{T}_0(\vec{r}_\Sigma;\tau)\hat{e}_T}{|\hat{n} \times \hat{e}_z|^{\frac{1}{2}}} \right] \tag{3.22}$$

where we have integrated from zero to infinity in ξ and used the fact that $\tilde{\vec{V}}_1$ must approach zero as ξ approaches infinity.

Thus, the boundary-layer suction is solved to within a function that represents the boundary-layer temperature on the container, which must ultimately be determined from the given temperature distribution on the container.

First-Order Interior

Problem A3 describes the first-order interior flow and it is given by

$$\underline{\text{mass}} \qquad \nabla \cdot \vec{V}_1 = 0 \tag{3.23}$$

$$\underline{\text{mom}} \qquad \nabla p_1 - T_1 \hat{e}_z = - \frac{\partial \vec{V}_0}{\partial \tau} \tag{3.24}$$

$$\underline{\text{energy}} \qquad W_1 = - P_r \frac{\partial T_0}{\partial \tau} \tag{3.25}$$

with

$$\vec{V}_1 + \tilde{\vec{V}}_1 = 0 \text{ on } \Sigma \tag{3.26}$$

$$T_0 = 0 \text{ at } \tau = 0 \quad . \tag{3.27}$$

We now decompose the interior velocity vector into a component that is in the cross plane and a component that is normal to the cross plane. In other words, let

$$\vec{V} = \vec{v} + W \hat{e}_z \tag{3.28}$$

where $\vec{v}$ has no component in the z-direction by definition. Then define the two-dimensional gradient operator in the cross plane to be

$$\nabla_2 \equiv \left(\frac{\hat{e}_1}{h_1} \frac{\partial}{\partial X_1} + \frac{\hat{e}_2}{h_2} \frac{\partial}{\partial X_2} \right) \tag{3.29}$$

where X_1 and X_2 are arbitrary cross-plane coordinates with unit vectors $\hat{e}_1$ and $\hat{e}_2$ and scale factors h_1 and h_2. Of course we may express the cross-plane velocity in terms of these cross-plane coordinates as

$$\vec{v} = u \hat{e}_1 + v \hat{e}_2 \tag{3.30}$$

where u and v are the velocity components in the X_1 and X_2 directions respectively.

Thus, the two-dimensional curl of the cross-plane velocity may be written as

$$\nabla_2 \times \vec{v} = \frac{1}{h_1 h_2}\left(\frac{\partial}{\partial X_1} h_2 v - \frac{\partial}{\partial X_2} h_1 u\right) \hat{e}_z \quad . \tag{3.31}$$

Furthermore, the total velocity, $\vec{\omega}$, is seen to be

$$\begin{aligned}\vec{\omega} &\equiv \text{curl } \vec{V} \\ &= \frac{1}{h_1 h_2}\left[h_1\left(\frac{\partial W}{\partial X_2} - \frac{\partial}{\partial z} h_2 v\right) \hat{e}_1 - h_2\left(\frac{\partial W}{\partial X_1} - \frac{\partial}{\partial z} h_1 u\right) \hat{e}_2\right. \\ &\qquad \left. + \left(\frac{\partial}{\partial X_i} h_2 v - \frac{\partial}{\partial X_2} h_1 u\right) \hat{e}_z\right] \quad .\end{aligned} \tag{3.32}$$

Hence, we are able to deduce the important result

$$\hat{e}_z \cdot \vec{\omega} = |\nabla_2 \times \vec{v}| \quad . \tag{3.33}$$

In other words, the magnitude of the cross-plane vorticity is equal to the z-component of the total vorticity to every order. But, as was seen from Eq. (2.100), this component of the total vorticity is zero for all time and to all orders. Thus, we conclude that the cross-plane velocity is irrotational in the cross plane.

The continuity equation states that the total velocity vector has no divergence to all orders. As a direct consequence to this we may use Eq. (3.28) to write

$$\nabla_2 \cdot \vec{v} = - \frac{\partial W}{\partial z} \quad . \tag{3.34}$$

This can be interpreted as the continuity equation for a constant density two-dimensional flow in the cross plane with a source term due to the vertical motion into the cross plane.

The zeroth-order interior has no flow in the vertical direction, as shown by Eq. (3.3). Thus, the zeroth-order cross-plane velocity has not only zero two-dimensional curl but also zero two-dimensional divergence.

It follows that the zeroth-order flow is a potential flow in the cross plane. Furthermore, the normal component of the zeroth-order velocity vanishes on the container as seen from Eq. (3.4). Hence, the zeroth-order flow in the cross plane is described by the Neumann problem with a vanishing boundary condition. Green's theorem in the plane shows that the solution to this problem is that the cross-flow vanishes. Therefore, we conclude that the inviscid interior is motionless to zeroth order!

Since the first-order velocity has a nonzero vertical component, Eq. (3.34) for the first-order cross flow becomes

$$\nabla_2 \cdot \vec{v}_1 = - \frac{\partial W_1}{\partial z} \ . \tag{3.35}$$

We may integrate this expression over the cross-plane area, A, and use the energy equation, Eq. (3.25), to show that, like T_0, W_1 depends only on the vertical spatial coordinate. The result of this integration is

$$\iint_A \nabla_2 \cdot \vec{v}_1 \, dA = - A \frac{\partial W_1}{\partial z} \ . \tag{3.36}$$

Green's theorem in the plane may be used to convert the area integral into a line integral to yield

$$A \frac{\partial W_1}{\partial z} = - \oint_{\mathcal{C}_e} \vec{v}_1 \cdot \hat{n}^* \, ds \ . \tag{3.37}$$

The expression relating $\hat{n}$ and $\hat{n}^*$, Eq. (3.18), can be substituted into the above expression giving

$$A \frac{\partial W_1}{\partial z} = - \oint_{\mathcal{C}_e} \vec{v}_1 \cdot \left[\frac{\hat{n} - (\hat{n} \cdot \hat{e}_z) \hat{e}_z}{|\hat{n} \times \hat{e}_z|} \right] ds$$

$$= - \oint_{\mathcal{C}_e} \frac{\vec{v}_1 \cdot \hat{n}}{|\hat{n} \times \hat{e}_z|} \, ds$$

$$= - \oint_{\mathcal{C}_e} \frac{(\vec{V}_1 - W_1 \hat{e}_z) \cdot \hat{n}}{|\hat{n} \times \hat{e}_z|} \, ds \quad . \tag{3.38}$$

This may be rearranged as

$$A \frac{\partial W_1}{\partial z} + \left[\oint_{\mathcal{C}_e} \frac{-\hat{n} \cdot \hat{e}_z}{|\hat{n} \times \hat{e}_z|} \, ds \right] W_1 = - \oint_{\mathcal{C}_e} \frac{\vec{V}_1 \cdot \hat{n}}{|\hat{n} \times \hat{e}_z|} \, ds \quad . \tag{3.39}$$

Leibnitz's rule for differentiating an integral can be used to show that the line integral on the left side of this equation is nothing more than the derivative of the cross-plane area. This calculation is done in the appendix. The argument of the line integral on the right is directly related to the boundary-layer suction through the boundary condition given by Eq. (3.26), which can be rewritten as

$$\vec{V}_1 \cdot \hat{n} = - \tilde{\vec{V}}_1 \cdot \hat{n} \text{ on } \Sigma \quad . \tag{3.40}$$

These two results allow us to write Eq. (3.39) in terms of the boundary-layer suction as

$$\frac{\partial}{\partial z} (AW_1) = \oint_{\mathcal{C}_e} \tilde{\vec{V}}_1 \cdot \hat{n} \frac{ds}{|\hat{n} \times \hat{e}_z|} \quad . \tag{3.41}$$

This equation simply reflects the fact that the vertical flow-rate must decrease as fluid is taken from the interior by boundary-layer suction ($\tilde{\vec{V}}_1 \cdot \hat{n}$ negative) and vice versa if fluid is added by the boundary layer.

We may manipulate the line integral in Eq. (3.41) into a surface integral by writing

$$\frac{\partial}{\partial z} (AW_1) = \frac{\partial}{\partial z} \int_1^z \left[\oint_{\mathcal{C}_e} \tilde{\vec{V}}_1 \cdot \hat{n} \frac{ds}{|\hat{n} \times \hat{e}_z|} \right] dz$$

$$= - \frac{\partial}{\partial z} \int_z^1 \oint_{\mathcal{C}_e} \tilde{\vec{V}}_1 \cdot \hat{n} \frac{ds \, dz}{|\hat{n} \times \hat{e}_z|}$$

$$= -\frac{\partial}{\partial z}\iint_{\Sigma_T} \tilde{\vec{V}}_1 \cdot \hat{n}\, d\Sigma \tag{3.42}$$

where Σ_T is that portion of the container surface, Σ, that lies above $\mathcal{C}_e$ as shown in Figure (3.2).

Now we may write from Eq. (3.42)

$$\frac{\partial}{\partial z}\left\{AW_1 + \iint_{\Sigma_T} \tilde{\vec{V}}_1 \cdot \hat{n}\, d\Sigma\right\} = 0 \tag{3.43}$$

We eliminate W_1 in favor of T_0 by using Eq. (3.25) and substitute the expression for the boundary-layer suction given by Eq. (3.22) into Eq. (3.43) to obtain

$$\frac{\partial}{\partial z}\left\{AP_r \frac{\partial T_0}{\partial \tau} - \frac{1}{\sqrt{2}}\iint_{\Sigma_T} \hat{n} \cdot \nabla \times \left[\frac{\tilde{T}_0(\vec{r}_\Sigma;\tau)\,\hat{e}_T}{|\hat{n} \times \hat{e}_z|^{\frac{1}{2}}}\right] d\Sigma\right\} = 0 \quad . \tag{3.44}$$

Stoke's theorem may be applied to the surface integral in this expression to yield a line integral. Then we have

$$\frac{\partial}{\partial z}\left\{AP_r \frac{\partial T_0}{\partial \tau} - \frac{1}{\sqrt{2}}\oint_{\mathcal{C}_e} \tilde{T}_0(\vec{r}_\Sigma;\tau)\frac{ds}{|\hat{n} \times \hat{e}_z|^{\frac{1}{2}}}\right\} = 0 \quad . \tag{3.45}$$

We now make use of the fact that the temperature is specified on the container as given by Eq. (3.9), to write

$$\tilde{T}_0(\vec{r}_\Sigma;\tau) = T_\Sigma - T_0 \text{ on } \Sigma \quad . \tag{3.46}$$

Then the equation governing the zeroth-order interior temperature becomes

$$\frac{\partial}{\partial z}\left\{AP_r \frac{\partial T_0}{\partial \tau} - \frac{1}{\sqrt{2}}\oint_{\mathcal{C}_e} (T_\Sigma - T_0)\frac{ds}{|\hat{n} \times \hat{e}_z|^{\frac{1}{2}}}\right\} = 0 \quad . \tag{3.47}$$

This equation can be integrated to yield

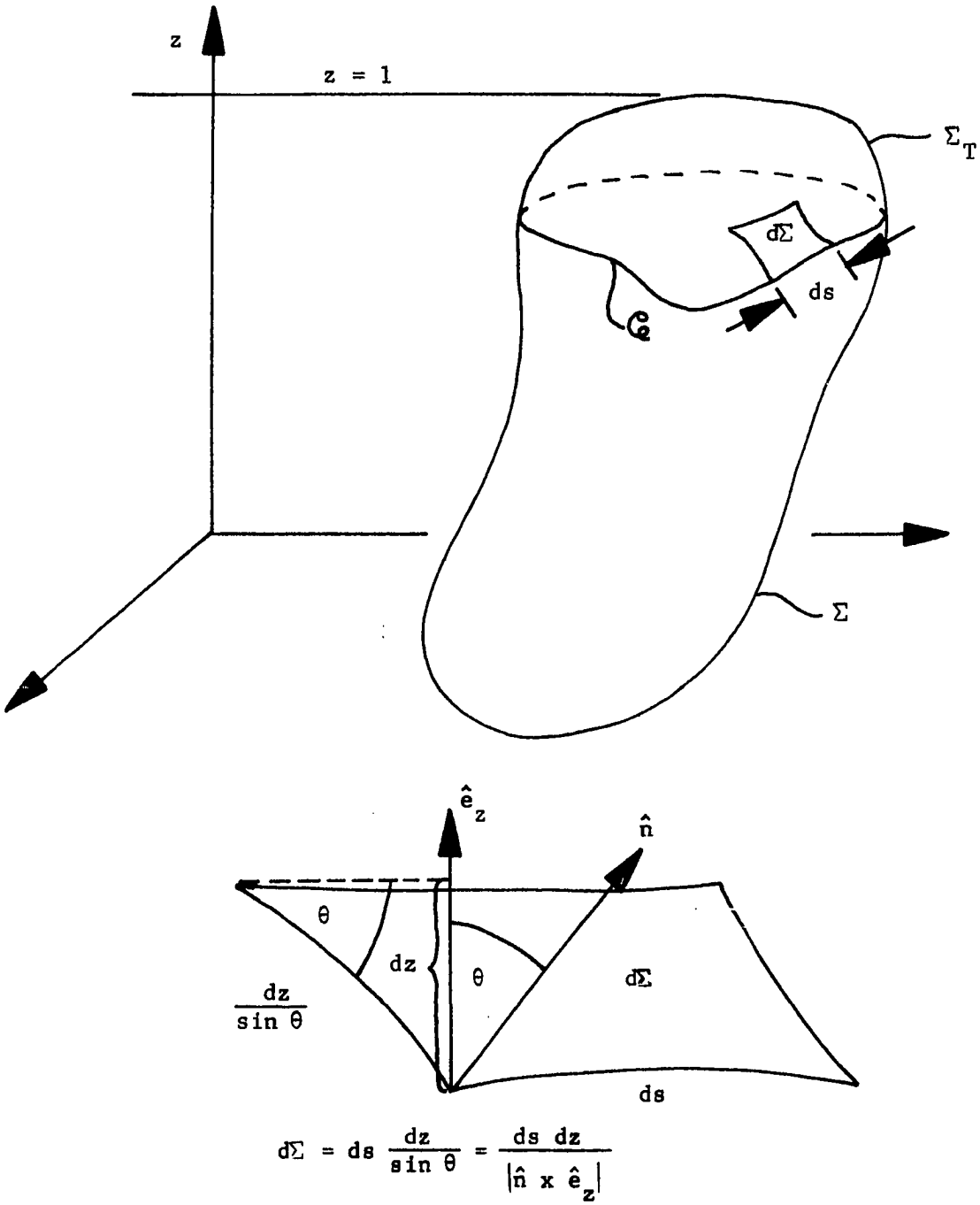

Figure 3.2 Surface Integral Geometry

$$AP_r \frac{\partial T_0}{\partial \tau} + \left[\frac{1}{\sqrt{2}} \oint_{\mathcal{C}_e} \frac{ds}{|\hat{n}x\hat{e}_z|^{\frac{1}{2}}}\right] T_0 = \frac{1}{\sqrt{2}} \oint_{\mathcal{C}_e} T_\Sigma \frac{ds}{|\hat{n}x\hat{e}_z|^{\frac{1}{2}}} + f(\tau) \qquad (3.48)$$

where $f(\tau)$ is the function of integration. Since T_Σ depends on spatial location and $f(\tau)$ does not, it is obvious that $f(\tau)$ is independent of T_Σ. That is, $f(\tau)$ is the same no matter what temperature boundary condition is imposed. Furthermore, if T_Σ remains zero for all time, then T_0 must remain zero for all time, which leads to the conclusion that $f(\tau)$ is identically zero. Hence, the solution to Eq. (3.48) can be obtained by use of the integrating factor as

$$T_0 \exp\left[\frac{1}{\sqrt{2}\,P_r} \frac{1}{A} \oint_{\mathcal{C}_e} \frac{ds}{|\hat{n} \times \hat{e}_z|^{\frac{1}{2}}} \tau\right] = \frac{1}{\sqrt{2}\,P_r} \frac{1}{A} \oint_{\mathcal{C}_e} T_\Sigma \frac{ds}{|\hat{n}x\hat{e}_z|^{\frac{1}{2}}} \frac{\exp\left[\frac{1}{\sqrt{2}\,P_r} \frac{1}{A} \oint_{\mathcal{C}_e} \frac{ds}{|\hat{n}x\hat{e}_z|^{\frac{1}{2}}} \tau\right]}{\frac{1}{\sqrt{2}\,P_r} \frac{1}{A} \oint_{\mathcal{C}_e} \frac{ds}{|\hat{n}x\hat{e}_z|^{\frac{1}{2}}}}$$

$$+ g(z) \qquad (3.49)$$

where $g(z)$ is the function of integration.

Let us define the "average" value of any variable Q around $\mathcal{C}_e$ to be

$$\langle Q \rangle \equiv \frac{\oint_{\mathcal{C}_e} Q \frac{ds}{|\hat{n} \times \hat{e}_z|^{\frac{1}{2}}}}{\oint_{\mathcal{C}_e} \frac{ds}{|\hat{n} \times \hat{e}_z|^{\frac{1}{2}}}} \qquad (3.50)$$

Thus the e-folding time, τ_H, can be defined to be

$$\tau_H = \sqrt{2}\, P_r \frac{A}{\mathcal{C}_e} \langle |\hat{n} \times \hat{e}_z|^{\frac{1}{2}} \rangle \qquad (3.51)$$

so that Eq. (3.49) can be rewritten as

$$T_0 = \langle T_\Sigma \rangle + g(z) \exp(-\tau/\tau_H) \quad . \qquad (3.52)$$

We may now apply the condition that T_0 is initially zero, given by Eq. (3.27), to obtain

$$g(z) = - < T_{\Sigma} > \quad . \tag{3.53}$$

Therefore, we can write the solution for the zeroth-order interior temperature to be

$$T_0 = < T_{\Sigma} > [1 - \exp(-\tau/\tau_H)] \quad . \tag{3.54}$$

The solution for the first-order vertical velocity component in the interior is given in terms of the time derivative of this temperature by the energy equation which is Eq. (3.25). This velocity component can be written as

$$W_1 = - \frac{P_r}{\tau_H} < T_{\Sigma} > \exp(-\tau/\tau_H) \tag{3.55}$$

after performing the time differentiation.

The nondimensional e-folding time, or "heat-up" time τ_H, can be written in terms of physical time as

$$t_H = \sqrt{2} \; \frac{A}{\mathcal{C}_e} \; \frac{P_r^{\frac{1}{2}} R_a^{\frac{1}{2}}}{N} \; < |\hat{n} \times \hat{e}_z|^{\frac{1}{2}} > \tag{3.56}$$

where t_H = dimensional heat-up time

A = horizontal cross-sectional area of the container nondimensionalized by L^2

$\mathcal{C}_e$ = circumference of A nondimensionalized by L

L = height of the container

N = Bunt-Väisälä frequency

P_r = Prandtl number

R_a = Rayleigh number.

To complete the solution to the general heat-up problem we must find the first-order interior flow in the cross plane. As we have already seen, the cross-plane velocity is irrotational in the cross plane, i.e.

$$\nabla_2 \times \vec{v}_1 = 0 \ . \tag{3.57}$$

Thus, we may derive the cross-plane velocity from a scalar potential by writing

$$\vec{v}_1 = \nabla_2 \varphi_1 \ . \tag{3.58}$$

But Eq. (3.35) gives

$$\nabla_2 \cdot \vec{v}_1 = - \frac{\partial W_1}{\partial z} \ . \tag{3.59}$$

Therefore the governing equation for the cross-plane velocity potential is Poisson's equation

$$\nabla_2^2 \varphi_1 = - \frac{\partial W_1}{\partial z} \ . \tag{3.60}$$

The boundary condition given by Eq. (3.40) is

$$\vec{V}_1 \cdot \hat{n} = - \tilde{\vec{V}}_1 \cdot \hat{n} \text{ on } \Sigma \tag{3.61}$$

which may be rewritten by means of Eq. (3.18) and Eq. (3.28) as

$$(\vec{v}_1 + W_1 \hat{e}_z) \cdot (|\hat{n} \times \hat{e}_z| \, \hat{n}^* + (\hat{n} \cdot \hat{e}_z)\hat{e}_z) = - \tilde{\vec{V}}_1 \cdot \hat{n} \text{ on } \Sigma \ . \tag{3.62}$$

In terms of the velocity potential, this may be expressed as

$$|\hat{n} \times \hat{e}_z| \, \frac{\partial \varphi_1}{\partial n^*} + (\hat{n} \cdot \hat{e}_z) W_1 = - \tilde{\vec{V}}_1 \cdot \hat{n} \text{ on } \mathcal{C} \ . \tag{3.63}$$

Hence, substituting for the boundary-layer suction from Eq. (3.22) gives the following problem for calculating the cross-plane flow:

$$\nabla_2^2 \varphi_1 = - \frac{\partial W_1}{\partial z} \tag{3.64}$$

$$\text{with } \left\{ \frac{\partial \varphi_1}{\partial n^*} = - \frac{(\hat{n} \cdot \hat{e}_z)}{|\hat{n} \times \hat{e}_z|} \, W_1 - \frac{1}{\sqrt{2}} \frac{\hat{n}}{|\hat{n} \times \hat{e}_z|} \cdot \nabla_{\mathcal{C}} \left\{ \frac{(T_\Sigma - T_0)\hat{e}_T}{|\hat{n} \times \hat{e}_z|^{\frac{1}{2}}} \right\} \text{ on } \mathcal{C} \right. \tag{3.65}$$

where we have used Eq. (3.9) to express $\tilde{T}_0(\vec{r}_\Sigma; \tau)$ in terms of T_Σ and T_0. Thus, we find that the flow in the cross plane is equivalent to the flow of a two-dimensional, constant density, irrotational fluid with a

uniform source distribution provided by the vertical velocity. The boundary condition reflects the fact that flow penetrates the cross-plane circumference due to changing cross-plane area and due to boundary-layer suction.

This completes the lowest-order solution to the general heat-up problem. The temperature and vertical velocity are completely specified in terms of the "average" value around $\mathcal{C}_2$ of the container temperature. The cross-flow solution follows from the above Poisson equation and associated boundary condition which, of course, will depend upon the particular container geometry and temperature boundary condition being considered.

Remarks

It is interesting to note that, unlike the usual external forced-convection boundary-layer theory, the theory of buoyancy-driven contained fluids has an inherent coupling between the inviscid region and the associated internal boundary layers. In other words, we cannot calculate the lowest-order interior motion, make a boundary layer correction, and then proceed to calculate the first-order interior, etc. Instead, each "interior-boundary layer" pair must be calculated simultaneously. For example, the equation for the zeroth-order interior temperature, Eq. (3.45), contains imbedded in it the zeroth-order boundary-layer temperature, which in turn is known only in terms of the interior temperature. This reflects the fact that the lowest-order inviscid flow is driven by the lowest-order boundary layer; a situation far different from the more familiar external forced convection problem.

We can also write the energy equation for the next higher order interior flow. It is given by

$$P_r \frac{\partial T_1}{\partial \tau} + W_2 = - \nabla^2 T_0 \tag{3.66}$$

We see that for the final steady state this equation becomes

$$W_2 = - \frac{d^2 \langle T_\Sigma \rangle}{dz^2} \tag{3.67}$$

From this equation we can note the difference between a flow that is driven by a boundary temperature that is linear in z and one that is driven by a nonlinear boundary temperature. In the first case, the vertical motion ceases when thermodynamic equilibrium is achieved and the boundary layers die out in the heat-up time. In the second case, the final steady temperature profile is incompatible with a state of static equilibrium and although the lowest-order vertical motion ceases in the heat-up time the next higher order vertical velocity component, W_2, obviously does not.

CHAPTER IV

APPLICATION OF THE THEORY

Preliminary Remarks

The solution to the general problem of heat-up from a state of rest of a Boussinesq fluid in an arbitrarily shaped closed container is complete as far as the lowest-order temperature and vertical velocity are concerned. Given a particular container geometry and temperature boundary condition, one may immediately write down the solutions for temperature and vertical velocity in terms of the heat-up time, τ_H, and the "average" value of the boundary temperature, $< T_\Sigma >$.

This "average" value is taken around the perimeter, $\mathcal{C}_\ell$, of the cross-plane area, A, where the cross plane is defined to be that cross-sectional area of the container that is formed by intersecting the container with a plane of constant gravitational potential. This average is somewhat peculiar in that it is taken with respect to the weighting factor $|\hat{n} \times \hat{e}_z|^{-\frac{1}{2}}$, where $\hat{n}$ is defined as the outward pointing unit vector normal to the container and $\hat{e}_z$ is the unit vector in the direction of increasing gravitational potential as shown in Figure (4.1).

Mathematically, this "average" value for any quantity, Q, may be written as

$$< Q > = \frac{\oint_{\mathcal{C}_\ell} Q \, \frac{ds}{|\hat{n} x \hat{e}_z|^{\frac{1}{2}}}}{\oint_{\mathcal{C}_\ell} \frac{ds}{|\hat{n} x \hat{e}_z|^{\frac{1}{2}}}} . \qquad (4.1)$$

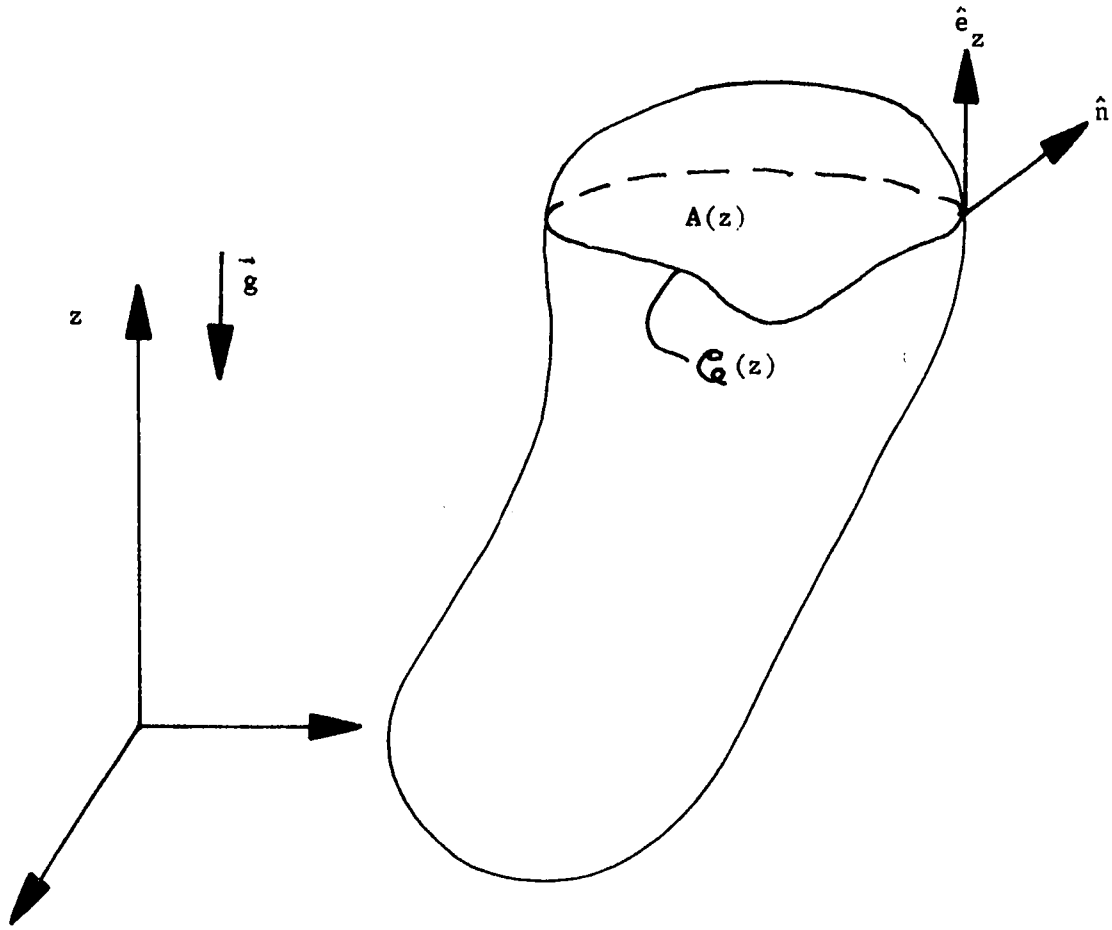

Figure 4.1 Heat-Up Geometry

The solution for the lowest-order temperature, T_0, and the lowest-order vertical velocity component, W_1, are, for any container geometry and temperature boundary condition, simply

$$T_0 = \langle T_\Sigma \rangle \left[1 - \exp(-\tau/\tau_H)\right] \tag{4.2}$$

$$W_1 = -\frac{P_r}{\tau_H} \langle T_\Sigma \rangle \exp(-\tau/\tau_H) \tag{4.3}$$

where $$\tau_H \equiv \sqrt{2}\ P_r \frac{A}{\mathcal{C}_Q} \langle |\hat{n} \times \hat{e}_z| \rangle^{\frac{1}{2}} \tag{4.4}$$

and P_r is the Prandtl number.

Eq. (4.2) shows that the inviscid interior temperature varies only with vertical position within the container and that this interior temperature approaches the average value of the container temperature asymptotically in time. Furthermore, we see from Eq. (4.3) that the vertical component of velocity in the interior approaches zero asymptotically in time. Thus, if there is any motion at all in the final steady state, that motion must be purely horizontal. This tendency toward horizontal flow is a characteristic of all stratified fluids and is often referred to as "plugging" or "plugged" flow. This phenomenon may be predicted by simply inspecting the linearized energy equation given by Eq. (2.69). This equation shows that W is identically zero in the inviscid interior when the fluid is at steady state.

The solution for the irrotational flow in the cross plane is not as straightforward since it involves solving the appropriate Poisson equation for each particular container geometry and temperature boundary condition that is considered. This Poisson equation is given by

$$\nabla_2^2 \varphi_1 = -\frac{\partial W_1}{\partial z} \tag{4.5}$$

with boundary condition

$$\frac{\partial \varphi_1}{\partial n^*} = - \frac{(\hat{n}\cdot\hat{e}_z)}{|\hat{n}x\hat{e}_z|^{\frac{1}{2}}} W_1 - \frac{1}{\sqrt{2}} \frac{\hat{n}}{|\hat{n}x\hat{e}_z|} \cdot \nabla x \left[\frac{(T_\Sigma - T_0)\hat{e}_T}{|\hat{n}x\hat{e}_z|^{\frac{1}{2}}} \right] \text{ on } \mathcal{C}. \tag{4.6}$$

The solution to this problem is the cross-flow velocity potential which is defined such that the lowest-order total velocity vector may be written as

$$\vec{V}_1 = \nabla_2 \varphi_1 + W_1 \hat{e}_z \ . \tag{4.7}$$

For this cross-flow problem, we have defined the gradient and Laplacian operators to be the appropriate two-dimensional operators in the cross plane. In other words,

$$\nabla_2 \equiv \left(\frac{\hat{e}_1}{h_1} \frac{\partial}{\partial X_1} + \frac{\hat{e}_2}{h_2} \frac{\partial}{\partial X_2} \right) \tag{4.8}$$

$$\nabla_2^{\,2} \equiv \left(\frac{\partial}{\partial X_1} \frac{h_2}{h_1} \frac{\partial}{\partial X_1} + \frac{\partial}{\partial X_2} \frac{h_1}{h_2} \frac{\partial}{\partial X_2} \right) \tag{4.9}$$

where X_1 and X_2 are cross-plane coordinates with unit vectors $\hat{e}_1$ and $\hat{e}_2$ and scale factors h_1 and h_2 as shown in Figure (4.2). As also shown in the figure, $\hat{n}^*$ is the outward pointing unit vector normal to $\mathcal{C}$ in the cross plane.

The cross-flow problem, as defined by the elliptic equation given by Eq. (4.5) with the boundary condition given by Eq. (4.6), is a well-posed problem whose solution for any container geometry and temperature perturbation is straightforward. Furthermore, there are special situations for which closed-form analytic solutions can be found. We will now attempt to reveal the important physical notions associated with various container geometries and boundary temperatures by treating several of these analytical examples.

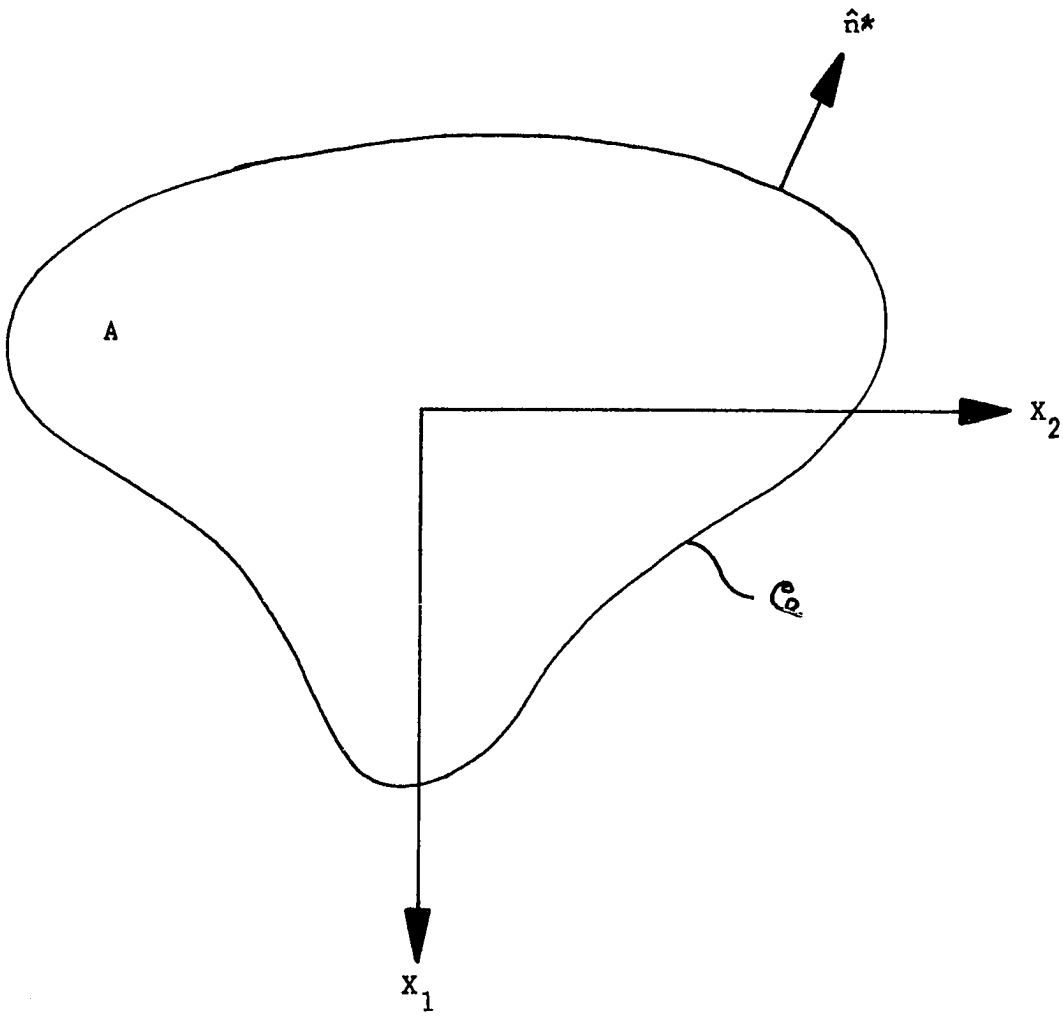

Figure 4.2 Cross-Plane Geometry

Right Cylinders

Let us consider the special class of containers consisting of right vertical cylinders of arbitrary cross section. That is, let the container have vertical sidewalls with horizontal ends, and let the horizontal cross section of this container have any arbitrary shape, as long as this shape is invariant from top to bottom as shown in Figure (4.3). For this class of containers we have the two conditions given by

$$\hat{n} \cdot \hat{e}_z = 0 \tag{4.10}$$

$$|\hat{n} \times \hat{e}_z| = 1 \quad . \tag{4.11}$$

In this case, Eq. (4.1) yields the result

$$< T_\Sigma > = \frac{1}{\mathcal{C}_e} \oint_{\mathcal{C}_e} T_\Sigma \, ds \tag{4.12}$$

which we recognize as the conventional average value of T_Σ around $\mathcal{C}_e$. Furthermore the heat-up time is a constant given by Eq. (4.4) to be

$$\tau_H = \sqrt{2} \, P_r \frac{A}{\mathcal{C}_e} \quad . \tag{4.13}$$

Thus, the temperature and vertical velocity solutions for all right vertical cylinders are given by Eq. (4.2) and Eq. (4.3) as

$$T_0 = < T_\Sigma > [1 - \exp(-\tau/\tau_H)] \tag{4.14}$$

$$W_1 = -\frac{1}{\sqrt{2}} \frac{\mathcal{C}_e}{A} < T_\Sigma > \exp(-\tau/\tau_H) \tag{4.15}$$

where $< T_\Sigma >$ is the conventional average value of the boundary temperature around the container perimeter, $\mathcal{C}_e$, and τ_H is a constant that depends on Prandtl number and the ratio of the container's cross-sectional area to its perimeter.

The cross-flow problem for all right vertical cylinders simplifies somewhat to

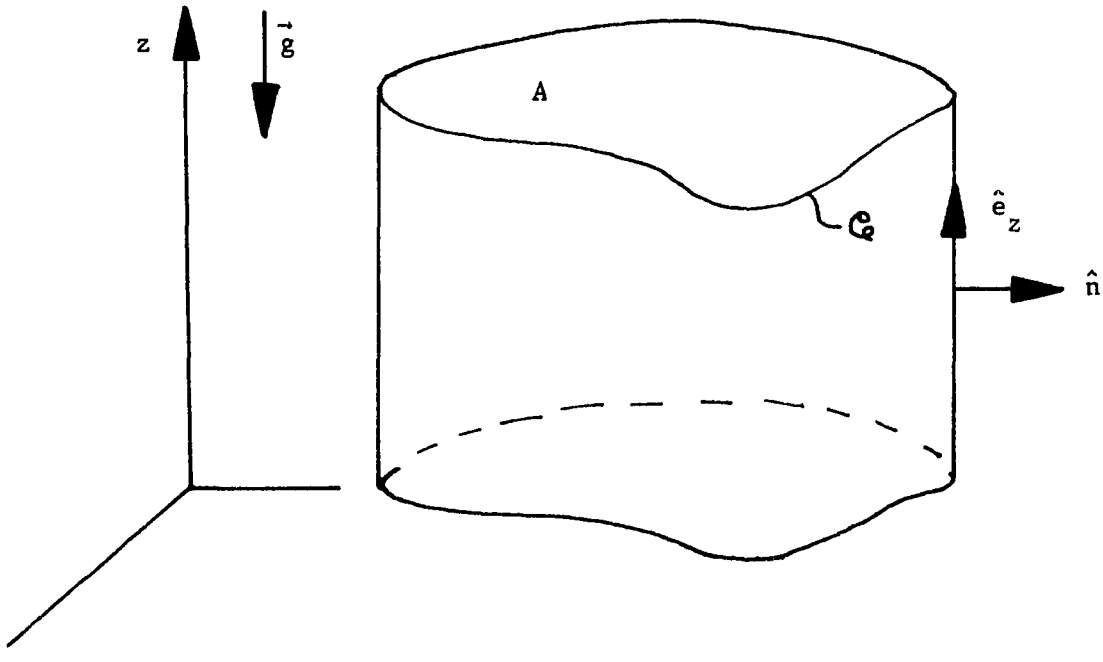

Figure 4.3 Right Cylinder

$$\nabla_2^2 \varphi_1 = \frac{1}{\sqrt{2}} \frac{\mathcal{C}_\ell}{A} \frac{\partial}{\partial z} < T_\Sigma > \exp(-\tau/\tau_H) \tag{4.16}$$

$$\text{with} \begin{cases} \frac{\partial \varphi_1}{\partial n} = -\frac{1}{\sqrt{2}} \hat{n} \cdot \nabla \times [(T_\Sigma - <T_\Sigma> + <T_\Sigma> \exp(-\tau/\tau_H))\hat{e}_T] \text{ on } \mathcal{C}_\ell \\ \end{cases} . \tag{4.17}$$

From this problem for flow in the cross plane we deduce the important result that the final steady state motion in the cross plane is always zero to lowest order unless the temperature boundary condition varies around the cross-plane perimeter, $\mathcal{C}_\ell$. In other words, as $\tau \to \infty$ we have

$$\nabla_2^2 \varphi_1 \to 0 \tag{4.18}$$

$$\text{and} \begin{cases} \frac{\partial \varphi_1}{\partial n} \to -\frac{1}{\sqrt{2}} \hat{n} \cdot \nabla \times [(T_\Sigma - <T_\Sigma>)\hat{e}_T] \text{ on } \mathcal{C}_\ell . \end{cases} \tag{4.19}$$

This equation describes a nonzero motion only when T_Σ differs from its average values around $\mathcal{C}_\ell$. Thus, a steady nonzero cross flow results only if the prescribed container temperature perturbation varies around the perimeter of the container.

Circular Cross Section

If we specialize the cross section of the right vertical cylinder of height L to be a circle of radius, R, then the obvious choice for the cross-plane coordinate system is the polar coordinate system shown in Figure (4.4). Of course, the nondimensional cross-plane area, A, and its circumference, $\mathcal{C}_\ell$, are

$$A = \pi (R/L)^2 \tag{4.20}$$

$$\mathcal{C}_\ell = 2\pi (R/L) \quad . \tag{4.21}$$

Hence, the heat-up time, as given by Eq. (4.13), is

$$\tau_H = \frac{P_r}{\sqrt{2}} \frac{R}{L} \quad . \tag{4.22}$$

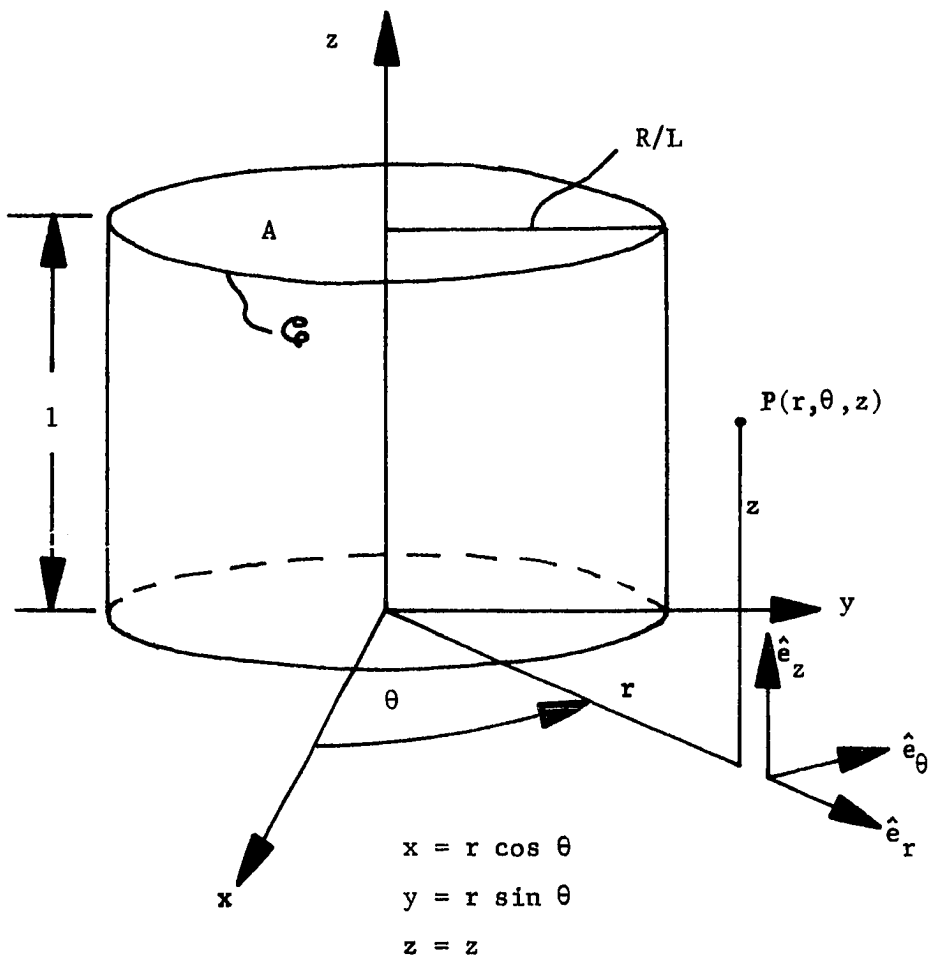

Figure 4.4 Right Circular Cylinder

z-Dependent Boundary Condition

Now assume that the given boundary temperature, T_Σ, depends only on the vertical spatial coordinate z, i.e.

$$T_\Sigma = T_\Sigma(z) \quad . \tag{4.23}$$

We refer to this as a z-dependent boundary condition in contrast to one which depends upon both z and some azimuthal coordinate. Since T_Σ does not vary around $\mathcal{C}_e$ it is obvious that the average value of T_Σ around $\mathcal{C}_e$ is equal to T_Σ itself. Of course, this can be seen directly from Eq. (4.12) and this can be expressed as

$$< T_\Sigma > = T_\Sigma \quad . \tag{4.24}$$

This result holds for any z-dependent boundary condition regardless of container geometry.

Thus, the temperature and vertical velocity solutions may be written down directly from Eq. (4.14) and Eq. (4.15) as

$$T_0 = T_\Sigma \left[1 - \exp(-\tau/\tau_H)\right] \tag{4.25}$$

$$W_1 = -\sqrt{2}\,\frac{L}{R}\,T_\Sigma \exp(-\tau/\tau_H) \tag{4.26}$$

where τ_H is given by Eq. (4.22). The Poisson problem becomes simply

$$\frac{1}{r}\frac{d}{dr}\left(r\frac{d\varphi_1}{dr}\right) = \sqrt{2}\;\frac{L}{R}\;\frac{dT_\Sigma}{dz}\exp(-\tau/\tau_H) \tag{4.27a}$$

$$\text{with}\quad \left\{\frac{d\varphi_1}{dr} = \frac{1}{\sqrt{2}}\;\frac{dT_\Sigma}{dz}\exp(-\tau/\tau_H)\ \text{ on } r = \frac{R}{L}\right. \tag{4.27b}$$

where we have reasoned that $\varphi_1 \neq \varphi_1(\theta)$ by symmetry arguments and reduced Eqs. (4.16) and (4.17) to this form.

The solution to this problem is found by a straightforward integration and application of the boundary condition to be

$$\frac{d\varphi_1}{dr} = \frac{1}{\sqrt{2}} \frac{L}{R} r \frac{dT_\Sigma}{dz} \exp(-\tau/\tau_H) \quad . \tag{4.28}$$

Then, if we write,

$$\vec{V}_1 = u_1\hat{e}_r + v_1\hat{e}_\theta + W_1\hat{e}_z \tag{4.29}$$

we obtain the following expressions for the velocity components

$$u_1 = \frac{1}{\sqrt{2}} \frac{L}{R} r \frac{dT_\Sigma}{dz} \exp(-\tau/\tau_H) \tag{4.30}$$

$$v_1 = 0 \tag{4.31}$$

$$W_1 = -\sqrt{2} \frac{L}{R} T_\Sigma \exp(-\tau/\tau_H) \tag{4.32}$$

where $$\tau_H = \frac{P_r}{\sqrt{2}} \frac{R}{L} \quad . \tag{4.33}$$

Since there is no flow in the azimuthal direction, it follows that the streamlines are along lines of constant θ. Hence, we see that the flow in the cross plane is purely in the radial direction and that the speed of this cross-plane flow increases with increasing distance from the center line of symmetry of the circular cylinder.

For the purpose of illustration, let us consider a boundary temperature that varies linearly in z with some arbitrary slope as shown in Figure (4.5). In terms of our normalization this translates into a boundary condition that is given by

$$T_\Sigma = m\left(z - \frac{m-1}{m}\right) \tag{4.34}$$

where m is a parameter which may be varied to describe linear profiles with various slopes.

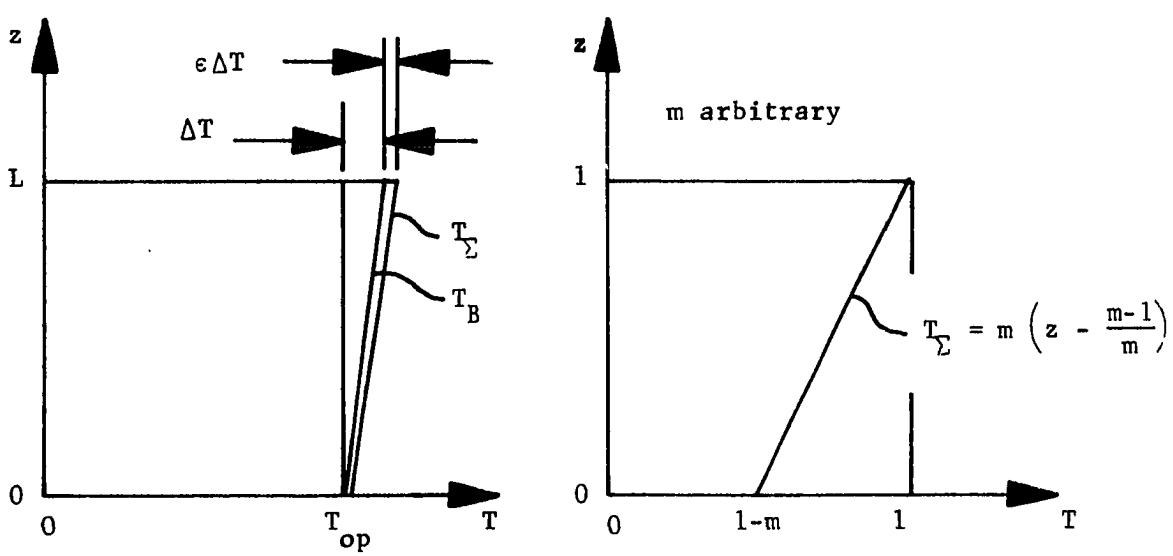

Figure 4.5 General Linear Boundary Condition

Then, for example, when m = 0 we have the temperature profile and quantitative flow pattern shown in Figure (4.6). Notice that dT_Σ/dz is zero in this case so that Eqs. (4.30) and (4.31) show that $u_1 = v_1 = 0$. Furthermore, Eq. (4.32) shows that W_1 is the same everywhere in the container at any given time. This is a pathological case for which there is no boundary-layer suction and hence no cross flow. The fluid simply rises near the hot container wall, producing a constant thickness vertical boundary layer, and settles in the inviscid interior until each fluid particle reaches a level at which its initial temperature equals the boundary temperature at that level. At this time the motion ceases, the boundary layer decays, and the fluid is heated.

There is no boundary-layer entrainment for the special case of flow in a vertical cylinder with a constant temperature perturbation, T_Σ. This is because the rate-of-change of vorticity in the boundary layer taken with respect to distance in the direction of boundary-layer flow is proportional to dT_Σ/dz for flow in a vertical cylinder with a z-dependent boundary condition. Hence, for a constant temperature perturbation, this rate-of-change of vorticity is zero. Thus, no vorticity is diffused out from the wall and a constant value of vorticity is convected along the vertical wall in a constant thickness boundary layer.

Although, in general, there will be boundary-layer suction, and thus a cross flow, this example does serve to illustrate the basic heat-up mechanism that typifies all of these contained flows. That mechanism is the boundary-layer driven convection in the inviscid interior that moves a constant temperature interior fluid particle from its initial level to its final level where its temperature matches the boundary temperature.

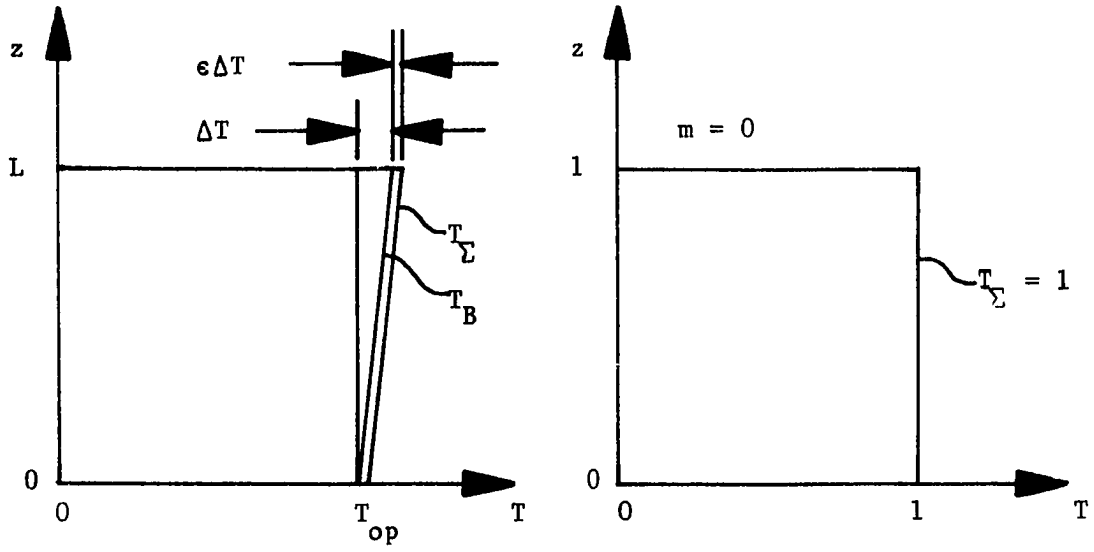

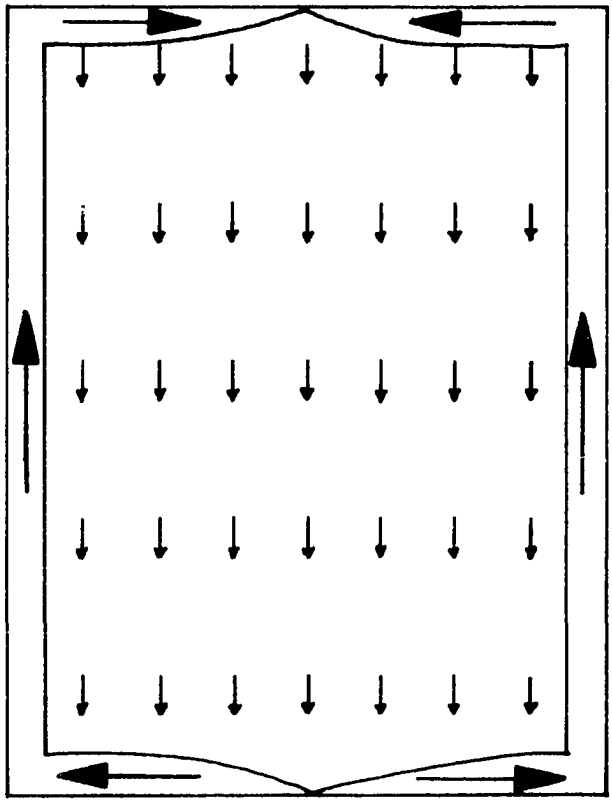

Cross Section Taken Thru $\mathbb{C}_L$

m = 0

Figure 4.6 Linear Boundary Temperature Producing Zero Boundary-Layer Suction

As a final example of a linear z-dependent boundary condition, consider the case where m = 2 as shown in Figure (4.7). Here the fluid rises near the hot wall (the upper half of the container) and falls near the cold wall (the lower half of the container). Hence, the fluid is always being entrained by the vertical boundary layers and they grow as shown. The interior convection is necessarily upward in the bottom half of the container and downward in the top half of the container in order to preserve conservation of mass. Hence, a "four-cell" pattern of flow develops as shown. This particular geometry and boundary condition was studied by Sakurai and Matsuda [10] by a different method and our solution agrees exactly with theirs in this case.

Azimuthally Varying Boundary Condition

Let us assume that the container temperature is known to be

$$T_\Sigma = f(z) \cos \alpha\theta \tag{4.35}$$

where α must be an integer so that T_Σ is single-valued. Then its average value, as given by Eq. (4.12), is

$$\langle T_\Sigma \rangle = \frac{1}{\mathcal{L}} \oint_{\mathcal{L}} f(z) \cos \alpha\theta \, ds$$

$$= \frac{f(z)}{2\pi} \oint_0^{2\pi} \cos \alpha\theta \, d\theta = 0 \quad . \tag{4.36}$$

This leads to the conclusion that

$$T_0 = 0 \tag{4.37}$$

$$W_1 = 0 \tag{4.38}$$

as seen from Eqs. (4.14) and (4.15). This result dramatizes what is apparent from inspecting Eqs. (4.14) and (4.15); namely, that the interior heat-up process is a response to the "average" value of the boundary

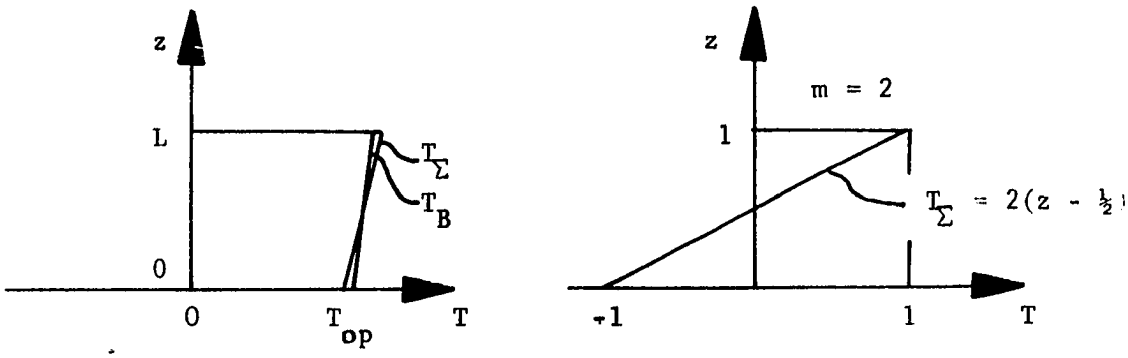

Physical Variables

Normalized Variables

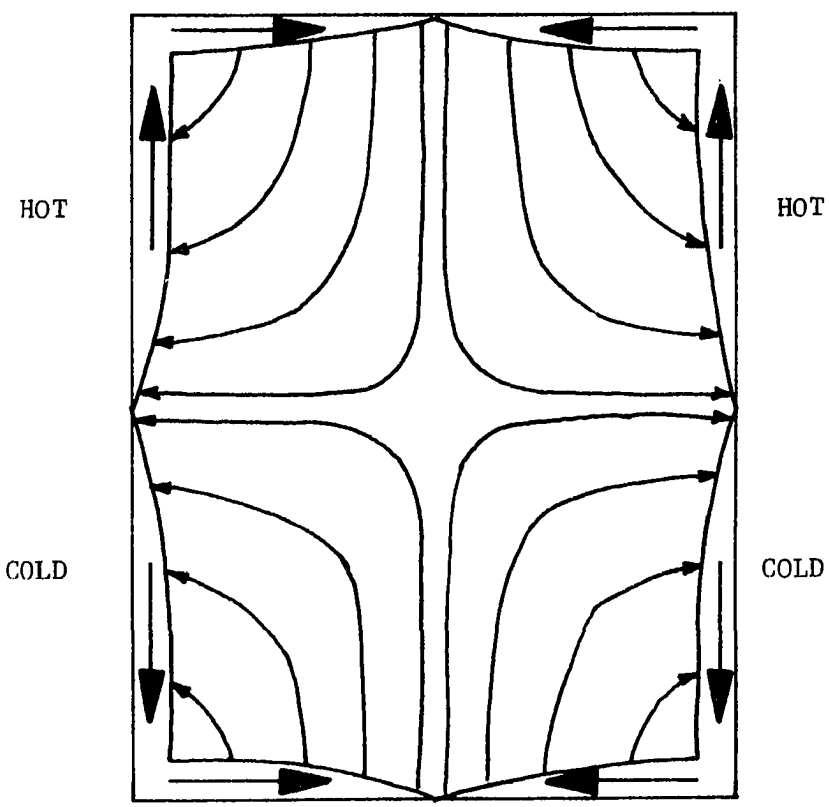

Cross Section Taken Thru $\mathcal{C}_L$

m = 2

Figure 4.7 Linear Boundary Temperature Producing Four-Cell Flow

temperature, and when that average is zero the fluid does not heat-up. However, this does not mean there is no cross flow. We can see this by inspecting the appropriate Poisson equation for this example, which reduces to

$$r^2 \frac{\partial^2 \varphi_1}{\partial r^2} + r \frac{\partial \varphi_1}{\partial r} + \frac{\partial^2 \varphi_1}{\partial \theta^2} = 0 \tag{4.39}$$

$$\text{with } \begin{cases} \dfrac{\partial \varphi_1}{\partial r} = \dfrac{f'(z)}{\sqrt{2}} \cos \alpha\theta \text{ on } r = \dfrac{R}{L} \end{cases} . \tag{4.40}$$

The solution to this problem can be easily obtained by the method of separation of variables as

$$\varphi_1 = \frac{f'(z)}{\sqrt{2}\,\alpha} \frac{r^\alpha}{(R/L)^{\alpha-1}} \cos \alpha\theta \quad . \tag{4.41}$$

This potential yields the following expressions for the velocity components:

$$u_1 = \frac{f'(z)}{\sqrt{2}} \left(\frac{r}{R/L}\right)^{\alpha-1} \cos \alpha\theta \tag{4.42}$$

$$v_1 = - \frac{f'(z)}{\sqrt{2}} \left(\frac{r}{R/L}\right)^{\alpha-1} \sin \alpha\theta \quad ; \quad \alpha = 1,2,3... \tag{4.43}$$

The equation for the streamlines of this cross flow is given by

$$\frac{dr}{u_1} = \frac{r d\theta}{v_1} \tag{4.44a}$$

which may be integrated to give the following equation for the streamlines.

$$r = \frac{\text{const}}{(\sin \alpha\theta)^{1/\alpha}} \quad . \tag{4.44b}$$

Then, for example, when $\alpha = 1$ and $f'(z)$ is positive we have the temperature profile and flow pattern shown in Figure (4.8). We see that

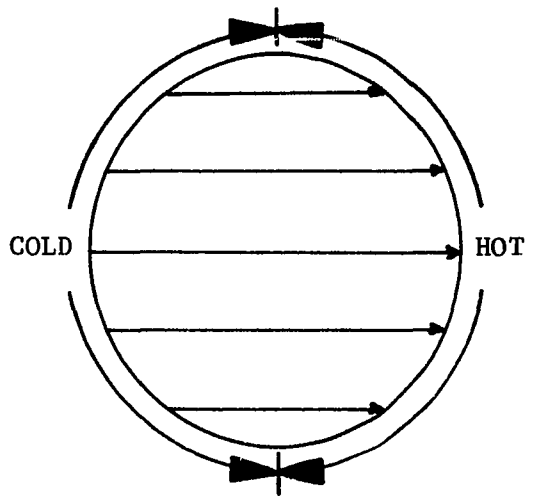

Top View of Interior Streamlines

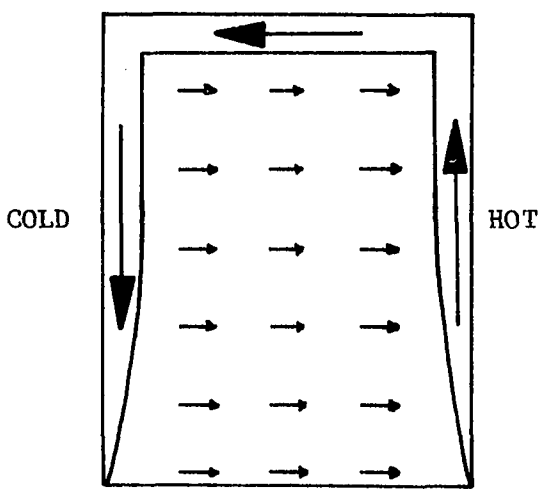

Cross Section Taken Thru $\mathcal{C}_L$

$T_\Sigma = f(z) \cos \theta$

Figure 4.8 Azimuthally-Varying Boundary Temperature Producing Plugged Flow

in this case a fluid particle rises in the boundary layer near the hot wall, crosses the top of the container in a horizontal boundary layer, descends in the boundary layer near the cold wall until it reaches its original level, and then crosses the interior of the container from the cold wall to the hot wall in a straightline motion that is often referred to as "plugging". This preference for purely horizontal motion in the interior (plugging) is often observed in steady natural convection problems.

The cross-flow pattern is shown in Figure (4.9) for the case when $\alpha = 2$ and $f'(z)$ is positive. This is an example of a different kind of four-cell motion than was depicted in Figure (4.7) for the z-dependent boundary condition.

As the parameter α increases through the integers, the flow will continue to divide into 2α cells in order for fluid to enter the interior at a cold wall and leave the interior at a hot wall. Notice that if $f'(z)$ is zero (that is, the boundary temperature varies only azimuthally and not with z) then not only is there no vertical motion but the cross flow is also zero as seen from Eqs. (4.42) and (4.43).

Although the form of the azimuthally varying boundary condition used in this example ($T_\Sigma = f(z) \cos \alpha\theta$) appears at first glance to be rather restrictive, it is actually quite general in that any arbitrary boundary condition can be Fourier synthesized by an infinite series that is composed of terms of this kind.

It is also worth mentioning at this point that the general solution to the cross-flow problem can be written in terms of a Neumann function which depends only on the geometry of the boundary curve $\mathcal{C}$.

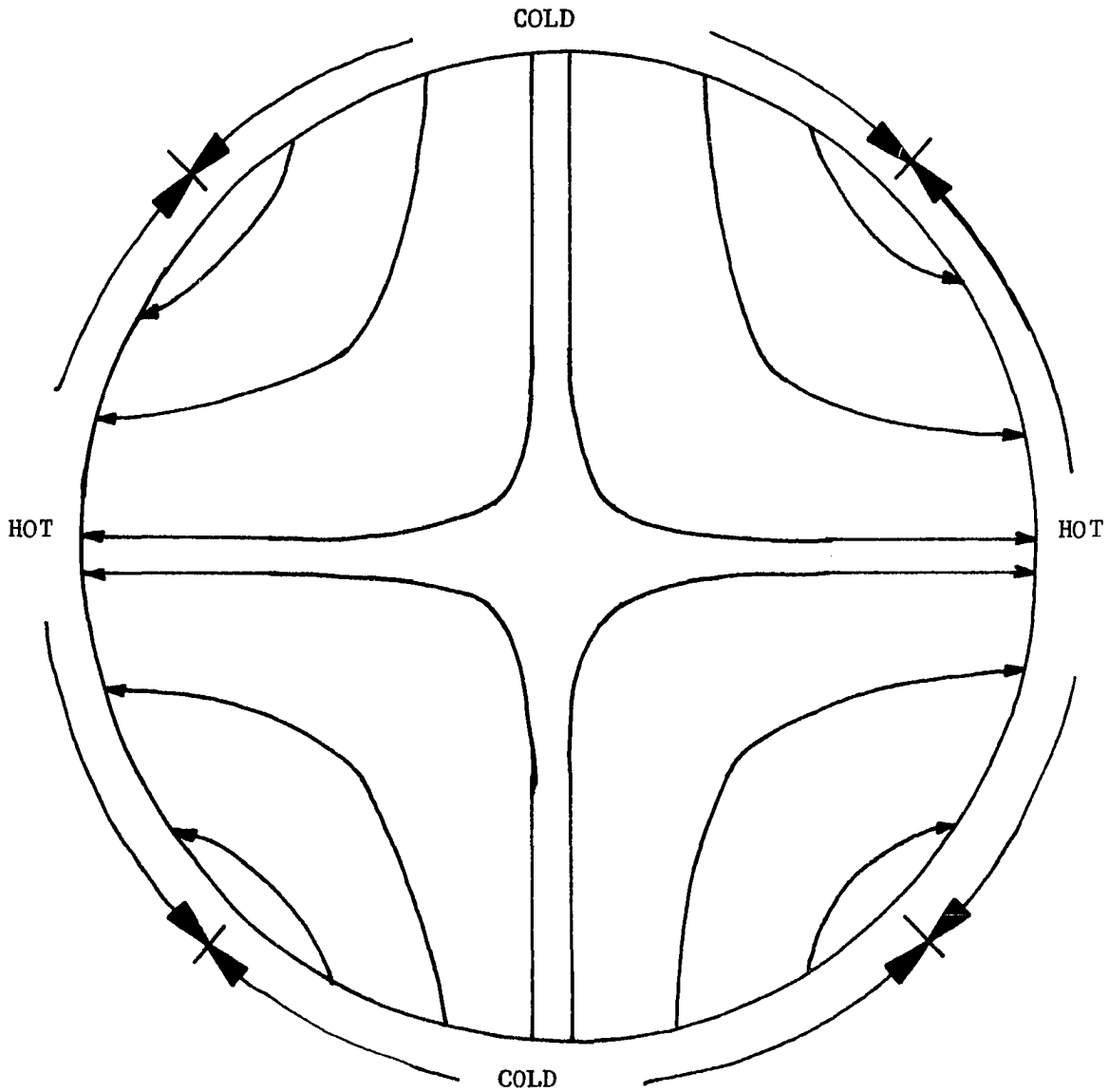

Top View of Interior Streamlines

$T_{\Sigma} = f(z) \cos 2\theta$

Figure 4.9 Azimuthally-Varying Boundary Temperature Producing Four-Cell Flow

This solution is

$$\varphi_1 = - \oint_{\mathcal{C}_Q} \frac{\partial \varphi_1}{\partial n^*} N \, ds \tag{4.45a}$$

where N is the Neumann function. The Neumann function must be determined from the following problem:

$$\nabla^2 N = - \frac{\partial W_1}{\partial z} N \tag{4.45b}$$

$$\text{with} \begin{cases} \dfrac{\partial N}{\partial n^*} = 0 \quad \text{on} \quad \mathcal{C}_Q & (4.45c) \\ N \sim - \dfrac{1}{2\pi} \log |\vec{r} - \vec{\zeta}| \quad \text{as} \quad \vec{r} \to \vec{\zeta} . & (4.45d) \end{cases}$$

Here $\vec{r}$ is the position vector as usual and $\vec{\zeta}$ is the position vector at a field point.

Thus, in principle, the solution for any geometry and any temperature perturbation is given by Eq. (4.45a) since $\partial \varphi_1 / \partial n^*$ on $\mathcal{C}_Q$ is known from Eq. (4.6) and the Neumann function can be found for a particular container geometry from the above problem. Of course, the Neumann function can be found analytically in very few cases and our discussion of simplified geometries and boundary conditions will continue. However, this general solution to the cross-flow problem may be useful in determining numerical solutions to more complicated problems and certainly emphasizes the elliptic behavior of the cross flow.

Elliptical Cross Section

Let the cross section of the right vertical cylinder of height L now be an ellipse with semi-major axis a and semi-minor axis b as shown in Figure (4.10). Now the obvious choice for the cross-plane coordinate system is the elliptic coordinate system also shown in the figure. The

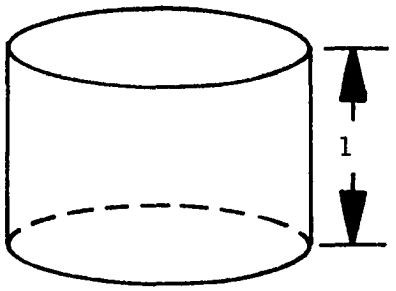

Elliptical Cylinder

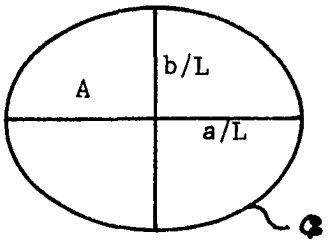

Top View

$$x = \alpha \cosh U \cos V$$

$$y = \alpha \sinh U \sin V$$

$$z = z$$

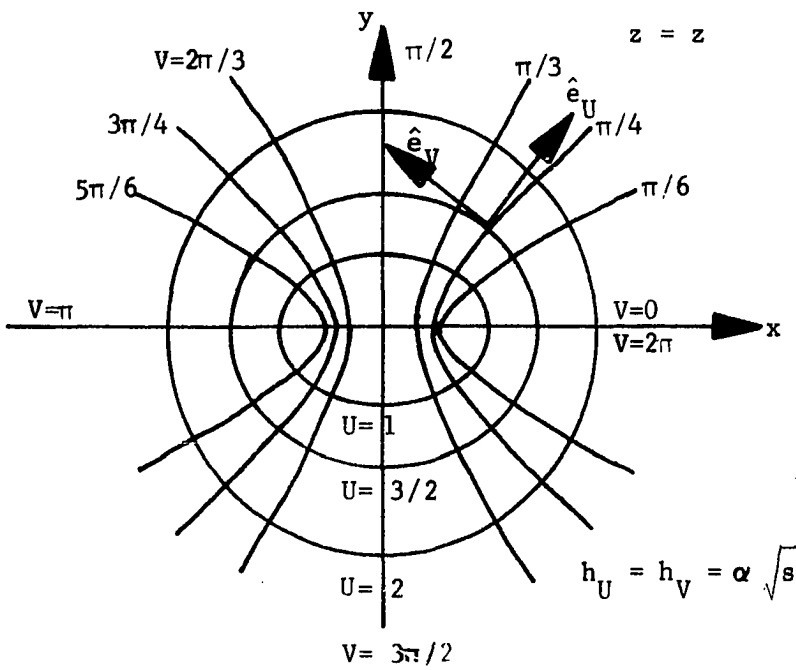

$$h_U = h_V = \alpha \sqrt{\sinh^2 U + \sin^2 V}$$

Elliptic Coordinate System

Figure 4.10 Right Elliptical Cylinder

nondimensional cross-plane area, A, and its circumference, $\mathcal{C}_{\mathcal{L}}$, are

$$A = \pi \frac{a}{L} \frac{b}{L} \tag{4.46}$$

$$\mathcal{C}_{\mathcal{L}} = 4 \frac{a}{L} \int_0^{\pi/2} \sqrt{1 - [1-(b/a)^2] \sin^2\theta} \, d\theta \tag{4.47a}$$

$$\approx 2\pi \sqrt{\frac{1}{2}\left[\left(\frac{a}{L}\right)^2 + \left(\frac{b}{L}\right)^2\right]} \, . \tag{4.47b}$$

The error in the approximation for the elliptic integral grows as the eccentricity of the ellipse increases. For instance, the expression for the circumference is exact for the limiting case of a circle (b/a = 1). The error in the approximation for the elliptic integral is less than three percent for b/a = 1/2 and grows to a maximum value of just over eleven percent as b/a approaches zero. Thus, the approximation is acceptable for most engineering work (especially for b/a greater than one half) and the convenience gained by avoiding elliptic integral tables justifies introducing the approximation.

The heat-up time (using the approximate perimeter) is

$$\tau_H = P_r \frac{\left(\frac{a}{L}\right)\left(\frac{b}{L}\right)}{\sqrt{\left(\frac{a}{L}\right)^2 + \left(\frac{b}{L}\right)^2}} \, . \tag{4.48}$$

With this expression, the lowest-order temperature and vertical velocity can be found from Eqs. (4.14) and (4.15).

It can be shown that the particular value of the elliptical coordinate U that describes the container is given by

$$U_\Sigma = \tanh^{-1}(b/a) \, . \tag{4.49}$$

Then, if we limit our attention to z-dependent boundary conditions, the problem for the cross flow reduces to

$$\nabla_2^2 \varphi_1 = \frac{P_r}{\tau_H} \frac{dT_\Sigma}{dz} \exp(-\tau/\tau_H) \tag{4.50}$$

with

$$\begin{cases} \dfrac{\partial \varphi_1}{\partial U} = \dfrac{1}{\sqrt{2}} \dfrac{dT_\Sigma}{dz} \exp(-\tau/\tau_H) \text{ on } U = U_\Sigma \end{cases} . \tag{4.51}$$

The solution to this equation is

$$\varphi_1 = \frac{C_\ell}{\sqrt{2}\,A} \frac{dT_\Sigma}{dz} e^{-\tau/\tau_H} \left[\frac{A}{C_\ell} \left(1 - \frac{C_\ell}{2\pi}\right) U + \frac{A}{4\pi} \frac{(\cosh^2 U - \sin^2 V)}{\cosh U_\Sigma \sinh U_\Sigma} \right] \tag{4.52}$$

where the condition that the cross-plane flow must be everywhere irrotational has been invoked in order to make the solution unique.

This expression for the velocity potential corresponds to the following cross-plane velocity components

$$u_1 = \frac{C_\ell}{\sqrt{2}\,A} \frac{dT_\Sigma}{dz} \frac{L}{b} \sinh U_\Sigma \, e^{-\tau/\tau_H} \left[\frac{\dfrac{A}{C_\ell}\left(1 - \dfrac{C_\ell}{2\pi}\right) + \dfrac{A}{2\pi} \dfrac{\cosh U \sinh U}{\cosh U_\Sigma \sinh U_\Sigma}}{\sqrt{\sinh^2 U + \sin^2 V}} \right] \tag{4.53}$$

$$v_1 = \frac{C_\ell}{\sqrt{2}\,A} \frac{dT_\Sigma}{dz} \frac{L}{b} \sinh U_\Sigma \, e^{-\tau/\tau_H} \left[\frac{-\dfrac{A}{2\pi} \dfrac{\sin V \cos V}{\cosh U_\Sigma \sinh U_\Sigma}}{\sqrt{\sinh^2 U + \sin^2 V}} \right] . \tag{4.54}$$

The governing differential equation for the cross-flow streamlines is

$$\frac{h_U dU}{u_1} = \frac{h_V dV}{v_1} . \tag{4.55}$$

This may be integrated to give the following streamline equation

$$\left[\frac{e^{2U} + 2\bar{A} - \sqrt{4\bar{A}^2 + 1}}{e^{2U} + 2\bar{A} + \sqrt{4\bar{A}^2 + 1}}\right]^{\left(\frac{1}{\sqrt{4\bar{A}^2 + 1}}\right)} = \frac{\text{const}}{\tan V} \tag{4.56}$$

where

$$\bar{A} \equiv \left(\frac{2\pi}{\mathfrak{C}_{\ell}} - 1\right) \cosh U_{\Sigma} \sinh U_{\Sigma} \quad . \tag{4.57}$$

Notice that we have the following three possibilities:

$$\bar{A} > 0 \qquad \text{for} \qquad \mathfrak{C}_{\ell} < 2\pi \tag{4.58}$$

$$\bar{A} = 0 \qquad \text{for} \qquad \mathfrak{C}_{\ell} = 2\pi \tag{4.59}$$

$$\bar{A} < 0 \qquad \text{for} \qquad \mathfrak{C}_{\ell} > 2\pi \quad . \tag{4.60}$$

Figure (4.11) shows the cross-flow streamline patterns for each of these three cases. When $\mathfrak{C}_{\ell}$ is less than 2π the streamlines tend to run parallel to the minor axis. When $\mathfrak{C}_{\ell}$ equals 2π the streamlines are straight lines emanating outward from the cylinder's centerline. When $\mathfrak{C}_{\ell}$ is less than 2π the streamlines tend to run parallel to the major axis of the ellipse. Inspection of Eq. (4.47b) shows that the approximate value of $\mathfrak{C}_{\ell}$ equals 2π when $(a^2+b^2)/2 = L^2$. Thus, the three separate cases arise due to a geometry effect that compares the size of the elliptical cross section with the height of the cylinder.

Ellipsoid of Revolution

Let us now consider the container to be an ellipsoid of revolution of height L and radius a as shown in Figure (4.12). We will introduce the polar coordinate system shown in the figure and take the radial coordinate r to be r_{Σ} on the container. The nondimensional cross-plane area and circumference are given by

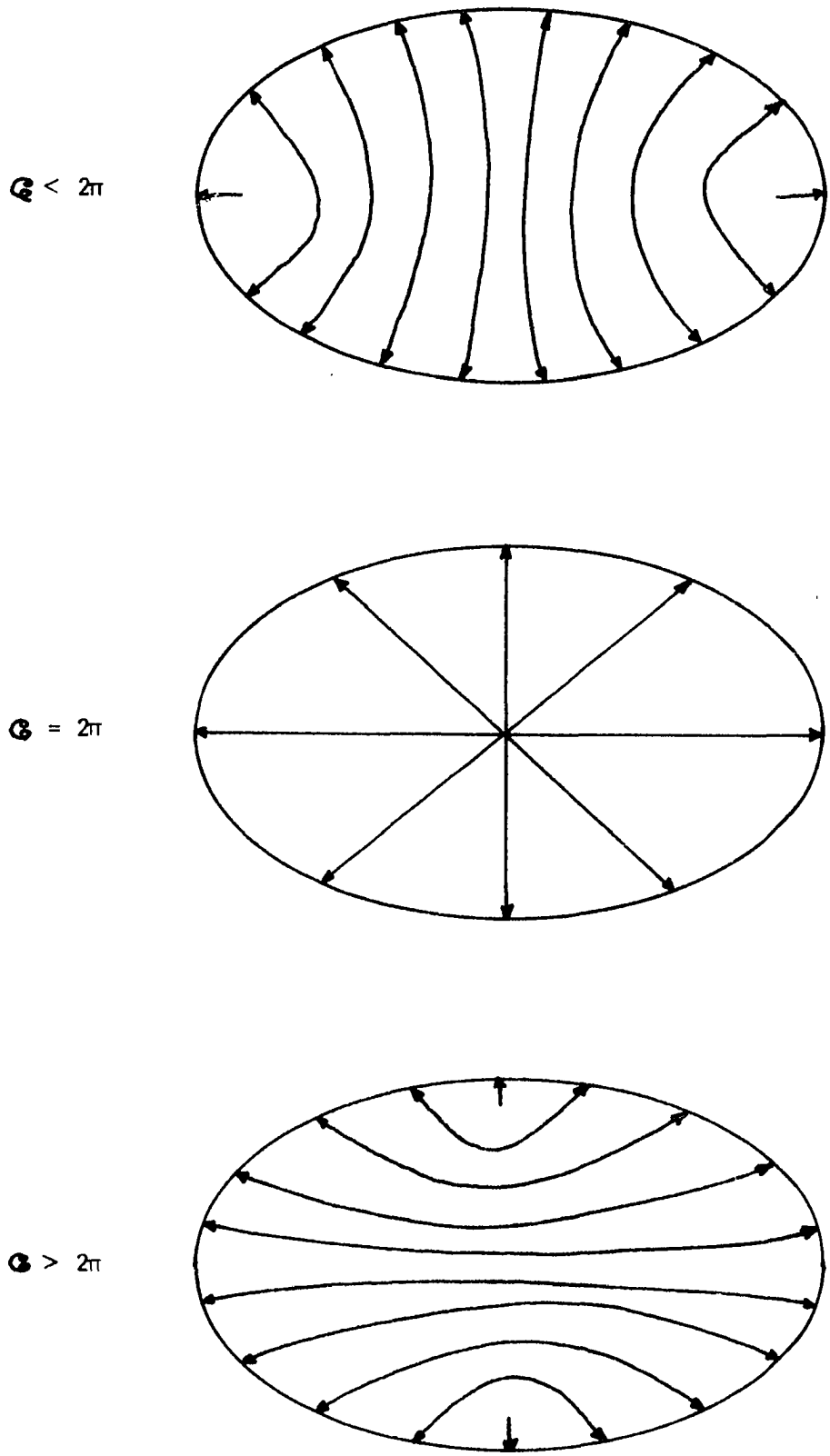

Figure 4.11 Cross-Flow Streamlines for a Right Elliptical Cylinder

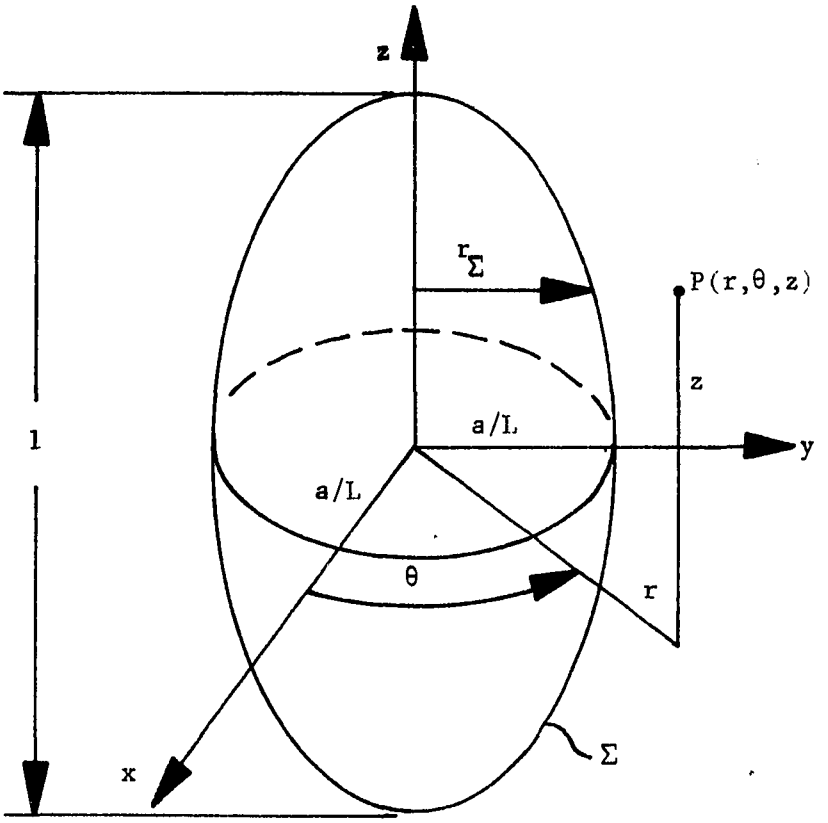

$$\frac{x^2}{(a/L)^2} + \frac{y^2}{(a/L)^2} + \frac{z^2}{(1/2)^2} = 1 \text{ on } \Sigma$$

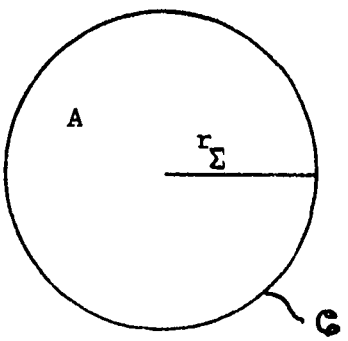

Top View at Arbitrary z

Figure 4.12 Ellipsoid of Revolution

$$A = \pi\, r_\Sigma^{\,2} \tag{4.61}$$

$$\mathcal{C}_\ell = 2\pi\, r_\Sigma \tag{4.62}$$

where $$r_\Sigma = \frac{a}{L}\sqrt{1 - 4z^2}\,. \tag{4.63}$$

The unit vector normal to the container is found to be

$$\hat{n} = \frac{r_\Sigma\, \hat{e}_r + 4\left(\frac{a}{L}\right)^2 z\, \hat{e}_z}{\sqrt{r_\Sigma^2 + 16\left(\frac{a}{L}\right)^4 z^2}}\,. \tag{4.64}$$

Therefore $< |\hat{n} \times \hat{e}_z|^{\frac{1}{2}} >$ is calculated as

$$< |\hat{n} \times \hat{e}_z|^{\frac{1}{2}} > = \sqrt[4]{\frac{1 - 4z^2}{1-4\left(1-4\left(\frac{a}{L}\right)^2\right)z^2}}\,. \tag{4.65}$$

Thus, the heat-up time, as given by Eq. (4.4), is

$$\tau_H = \frac{P_r}{\sqrt{2}}\,\frac{a}{L}\,\frac{(1-4z^2)^{3/4}}{\left[1-4\left(1-4\left(\frac{a}{L}\right)^2\right)z^2\right]^{1/4}} \tag{4.66}$$

And we see that, unlike the cylindrical case, the ellipsoidal heat-up time is not constant but varies with z.

If we consider the special case of the z-dependent boundary condition, then the Poisson equation for flow in the cross plane reduces to

$$\frac{1}{r}\frac{d}{dr}\left(r\,\frac{d\varphi_1}{dr}\right) = \frac{P_r}{\tau_H}\,\frac{dT_\Sigma}{dz}\; e^{-\tau/\tau_H} \tag{4.67}$$

with

$$\begin{cases} \dfrac{d\varphi_1}{dr} = \dfrac{r_\Sigma}{2}\,\dfrac{P_r}{\tau_H}\,\dfrac{dT_\Sigma}{dz}\, e^{-\tau/\tau_H} & \text{on } r = r_\Sigma \end{cases} \tag{4.68}$$

where we have assumed that $\varphi_1 \neq \varphi_1(\theta)$ by reason of symmetry. The solution to this problem, in terms of the velocity components, is

$$u_1 = \frac{P_r}{2} \frac{d}{dz} \left(\frac{T_\Sigma \, e^{-\tau/\tau_H}}{\tau_H} \right) r \tag{4.69}$$

$$v_1 = 0 \quad . \tag{4.70}$$

Recall that for a right circular cylinder of height L and radius R we found the heat-up to be given by Eq. (4.22) as

$$\tau_H(\text{cylinder}) = \frac{P_r}{\sqrt{2}} \frac{R}{L} \quad . \tag{4.71}$$

Thus, if we take Eq. (4.66) to give the heat-up time for an ellipsoid of revolution of height L and radius a, we can form the following comparison:

$$\left(\frac{R}{a}\right) \frac{\tau_{H(\text{ellipsoid})}}{\tau_{H(\text{cylinder})}} = \frac{(1-4z^2)^{3/4}}{\left[1-4\left(\frac{a}{L}\right)^2 z^2\right]^{1/4}} \quad . \tag{4.72}$$

A plot of this equation is shown in Figure (4.13). If the two containers are to have the same volume, then R/a must be taken to be the square root of two-thirds. If instead, the two containers are to have the same radius, then, of course, R/a is unity by definition. Notice that in both cases the height of the container is the same, namely L. As a/L increases, the cylinder's heat-up "advantage" decreases. That is, the "fatter" the ellipsoid, the faster the fluid in the ellipsoid heats-up in comparison with a circular cylinder of the same volume. Observe that an ellipsoid with a/L = 1/2 corresponds to a spherical container of diameter L.

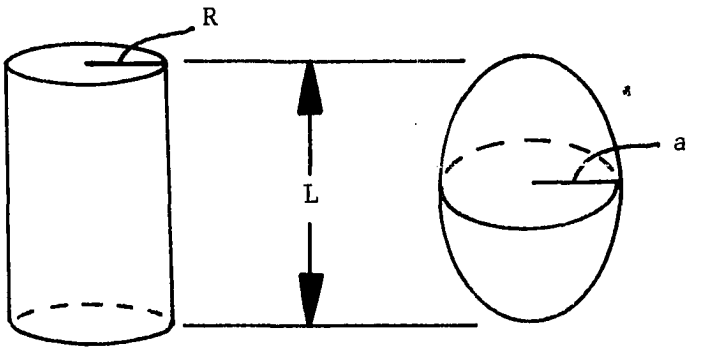

Note:

(1) R/a = 1 for equal height, equal width containers.

(2) R/a = $\sqrt{2/3}$ for equal height, equal volume containers.

(3) a/L = 1/2 is a sphere of radius L/2.

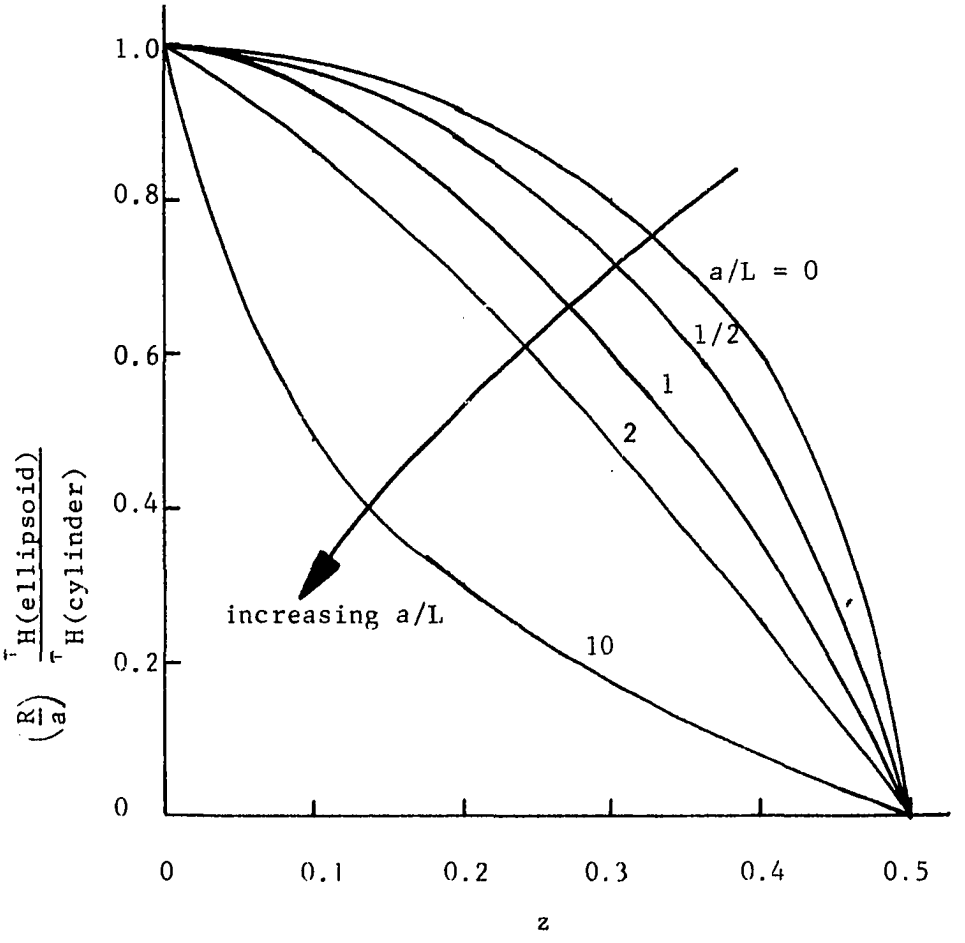

Figure 4.13 Heat-up Comparison Between a Cylinder and an Ellipsoid

The general heat-up solution will combine all of the features illustrated in the preceeding examples, When an arbitrarily shaped closed container is perturbed by a general impulsive boundary temperature, a boundary layer will be formed almost instantaneously. This boundary layer will entrain fluid from the inviscid interior establishing boundary-layer suction and consequently (because of mass conservation) vertical motion in the interior. Furthermore, the boundary layer will average azimuthal variations in the container temperature such that it presents an effective isothermal boundary to each horizontal layer of interior fluid. However, each horizontal layer of fluid in the interior is initially isothermal since the fluid originally is in a stratified state of static equilibrium. There is no mechanism for heat transfer in the interior other than convection. Thus, each horizontal layer of isothermal fluid will remain isothermal as it is convected to its new equilibrium position at a velocity whose vertical component is constant across each horizontal layer. The final heated state is approached asymptotically in time and the e-folding time for this heat-up process will vary with vertical location within the container. Finally, the interior fluid layer will (asymptotically) reach a level where the temperature of this layer equals the average container temperature and the fluid will have returned to thermal equilibrium with the container. "Net" boundary-layer entrainment will cease, as will vertical motion in the interior, and the fluid will be "heated". Horizontal motion (plugging) will persist, with fluid entering the interior at a "cold" wall and leaving the interior at a "hot" wall in such a way that the net mass flux into the interior is zero.

CHAPTER V

CONCLUSIONS AND RECOMMENDATIONS

Conclusions

The solution to the general linearized heat-up problem has been found. That is, given that a Newtonian, weakly-stratified fluid with constant fluid properties is initially at rest in a completely filled closed container of arbitrary shape, and given that the temperature of this container is impulsively changed by a "very small" amount, then the response of the fluid to this temperature perturbation is now known. The interior temperature and vertical velocity solutions are simply written in terms of the circumferential "average" value of the temperature perturbation. The flow in the cross plane must be determined by solving the appropriate Poisson equation for the particular temperature perturbation and container geometry being considered. However, this Poisson equation is well-posed and a numerical solution is straightforward.

It was found from the analysis that the inviscid interior region responds to a special "average" value of the temperature perturbation on the container and that the effect of the boundary layer is to smear out, or average, any circumferential variation in this perturbation so that the interior region, in effect, responds to an isothermal cross-plane boundary.

The heat-up mechanism is convective in nature. Conduction and viscosity are important only in thin boundary layers of thickness of the order

of $R_a^{-\frac{1}{4}}$ that lie near the container walls. These boundary layers become fully developed within a few periods of the Brunt-Väisälä frequency and then change very slowly during heat-up. The viscous boundary layer requires that a small mass flux be established in the interior region normal to the container sidewalls which in turn requires a small vertical mass flow in the interior in order to preserve continuity. This boundary-layer "suction" provides the basic heat-up mechanism. By this process, each interior fluid particle convects its "temperature" (more precisely, its static enthalpy) from its original equilibrium location to some new equilibrium location within the container where this temperature must necessarily equal the corresponding boundary temperature as shown in Figure (5.1). Thus, the fluid is heated-up, i.e. the interior temperature equals the "boundary" temperature (which is a boundary-layer-averaged container temperature) and the vertical motion ceases. Horizontal motion will persist if the container temperature has azimuthal variations. This is the "plugging" effect that is common in stratified flows.

Several analytical solutions to the Poisson equation for flow in the cross plane were found in order to illustrate the basic heat-up process and the alterations to this process that various combinations of the temperature perturbation and container geometry cause. This first calculation for the circular cylinder with a z-dependent boundary condition displays all of the physical ideas associated with the general heat-up problem and at the same time affords great mathematical simplification.

The circular cylinder with an azimuthally varying boundary condition demonstrates explicitly the concept that the fluid responds to the

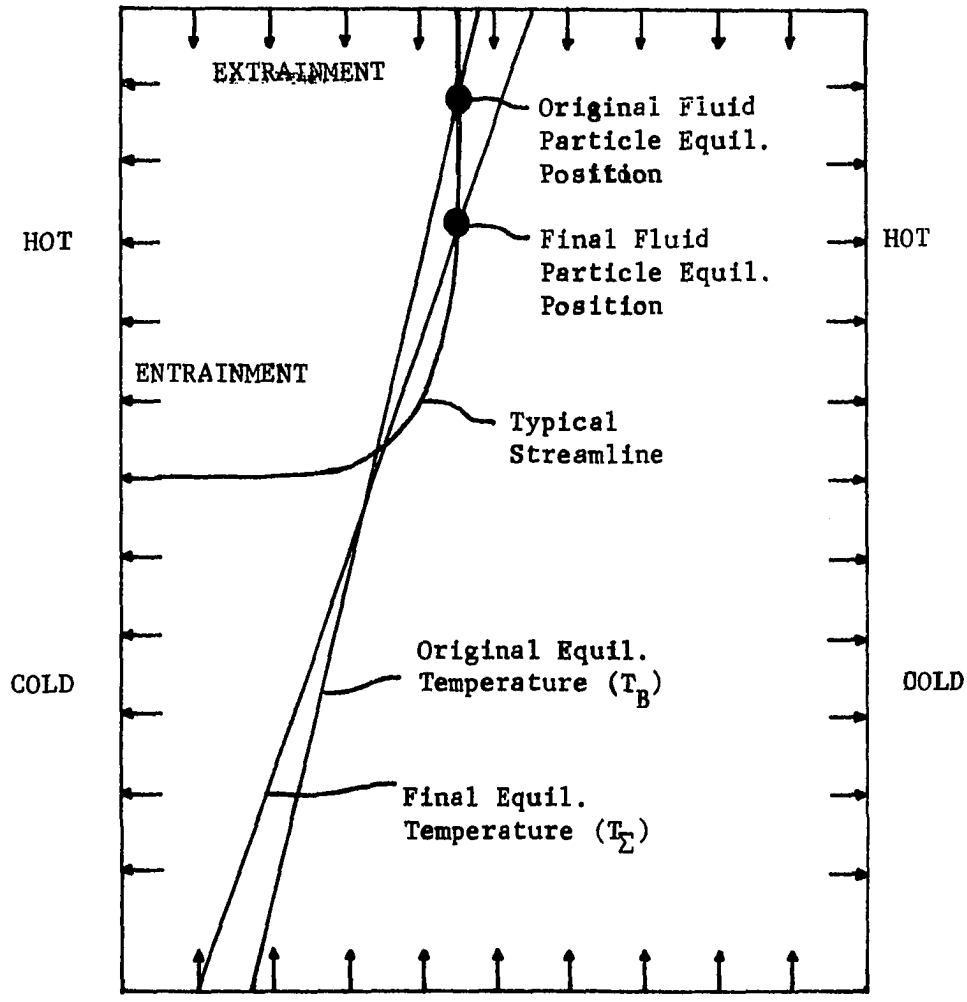

Figure 5.1 Interior Heat-up Mechamism

"average" temperature by showing that the interior temperature does not change for a sinusoidal azimuthal perturbation, since the average value of this perturbation is zero. Furthermore, we see that the cross flow is not zero for this case; instead it is the familiar "plugged" flow found in many stratified fluid problems.

The elliptical cylinder exhibits an odd "change-of-preference-for-flow-direction" that is dictated by a parameter that compares the (normalized) cross-sectional area of the cylinder with its (normalized) perimeter. This result warns that the effects associated with non-circular geometry are not safely dealt with by intuition. The calculation for the ellipsoid primarily demonstrates the fact that the heat-up time varies with vertical position for non-cylindrical containers.

The arbitrarily-shaped container was found to approach its final steady state asymptotically in time and thus the "heat-up" time was defined to be the e-folding time whose value was established to be proportional to $R_a^{\frac{1}{4}}$. Therefore, referring to Eq. (3.51), the insulating air gap in a pane of thermal glass heats-up in approximately two seconds, a two foot radius LOX fuel tank in a spacecraft on the pad heats-up in an hour and a half, a hundred foot diameter LNG storage tank heats-up in two days and the core of the Earth heats-up in about 10^9 years. The calculation for the Earth's core is based on data that is sketchy at best. Furthermore, the Prandtl number in the core is very large and consequently the viscous dissipation term should not be neglected as was done in our theory. Nonetheless, our calculation shows the danger of assuming that the core of the Earth is at steady state in continental drift calculations.

In our work we have assumed that the temperature on the container changes impulsively in time from a function that varies with location on

the container only (the basic stratification) to some new function that also only depends on position as seen from Eq. (2.71). In other words, the boundary temperature is assumed to be independent of time except during that initial instant in which it is impulsively perturbed. Nevertheless, if the boundary temperature varies slowly in time (on the heat-up time scale of order $R_a^{\frac{1}{4}}$) then the solution to this more general problem may be found from our theory by treating this time-varying boundary condition as an infinite number of impulsive jumps. This leads to the solution of the more general problem in terms of the so-called "superposition integral" as discussed in Hildebrand [21]. Observe that this more general solution is possible since the governing equations are linear (hence superposition is valid) and since a boundary condition that varies only on the slow heat-up time scale will drive a flow that is adequately described in terms of this slow time variation. Of course, boundary conditions that vary on a shorter time scale (on the order of the Brunt-Väisälä frequency) cannot be treated by this method and further investigation is necessary in this case. However, many time-varying boundary conditions do vary on the heat-up time scale, as seen in the preceeding paragraph. In particular, the diurnal variation (twenty-four hour period) is adequately described by this superposition solution for all examples mentioned above except the Earth's core.

Recommendations for Future Research

By analogy with the initial value problem, or spin-up problem, treated by Greenspan [19] in rotating flow theory it is anticipated that the assumed form of the interior solutions given by Eqs. (2.74) through (2.77) will not be adequate to synthesize a completely arbitrary basic

state. In other words, if the basic state is not a state of rest the analogy suggests that, in addition to the mode studied in the present work which varies only on the heat-up time scale, there are an infinite number of modes that vary on the shorter time scale associated with the Brunt-Väisälä frequency. Greenspan calls these the inertial modes. Thus, an investigation is needed to determine what the analogous situation is for the heat-up problem when the basic state is not one of static equilibrium. Connected to this investigation will be the problem of how to synthesize boundary conditions that vary on the shorter time scale associated with these "inertial" modes.

Another interesting analog with the rotating flow theory suggests that there are certain container geometries for which monatonic, non-oscillatory heat-up solutions are not possible. In other words, for certain containers the spin-up solution does not tend asymptotically to a steady state but remains unsteady for all time. In rotating flow theory, a container that has no closed curves of constant height (such as a cylinder with nonparallel planar ends) contains fluid that does not tend asymptotically to a steady state. Rotating flow solutions of this type were examined by Rossby [22] in a geophysical context and the resulting "shedding vortex" wave solution bears his name. It is suspected that the analogous container in stratified flow theory is one for which the derivative of the cross-plane area, dA/dz, is discontinuous. The heat-up analysis carried out here tacitly assumes that this derivative is continuous in going from Eq. (3.39) to Eq. (3.41). Furthermore, experiments done by Bishop et al. [23] support this suspicion. Bishop enclosed air between two concentric spheres that were maintained at different

temperatures and observed the resulting flow pattern. He found that for "moderate" temperature differences the flow is unsteady and characterized by the formation and shedding of small vortex cells. The cross-plane derivative, dA/dz, is discontinuous for the area between concentric spheres and therefore the possibility that Bishop observed the "Rossby waves" of stratified flow theory is ripe for investigation.

Krane [9] gave an analytical treatment to the problem of nonlinear, steady, two-dimensional flow in a rectangular cavity with different vertical wall temperatures and adiabatic, horizontal walls. Due to the fact that the vertical wall boundary layers are nonsimilar, Krane resorted to a Von Karman integral solution for the vertical wall boundary-layer equations. This in turn required the core temperature profile to be chosen from experimentally observed data rather than by matching with the vertical wall boundary layers. Thus, an analytical solution to the appropriate linearized version of Krane's problem could assist in understanding the more difficult nonlinear problem as well as reveal the general features of the transient motion that leads to this steady two-dimensional flow.

Other logical extensions of the present work include the following:

(i) specify the heat transfer on the boundary instead of the temperature

(ii) treat a basic state that has a discontinuous stratification (such as found in a partially filled container or in a container storing several immiscible fluids)

(iii) perturb the gravity vector instead of the boundary temperature in order to drive a linearized buoyant motion.

Finally, it should be noted that there is much room for experimental work in the field of contained buoyant fluids. This work can

range all the way from simple flow visualization experiments and heat transfer measurements, up to the more sophisticated measurement of modal decay factors and natural frequencies.

REFERENCES

1. Ostrach, S., "Natural Convection in Enclosures," Advances in Heat Transfer, Vol. 8, Hartnett, J.P. and Irvine, T.F. eds., Academic Press, New York, 1972, pp. 161-227.
2. Bailey, T.E. and Fearn, R.F., "Analytical and Experimental Determination of Liquid-Hydrogen Temperature Stratification," Advances in Cryogenic Engineering, Vol. 9, Timmerhaus, K.D., ed., Plenum Press, New York, 1963, pp. 254-264.
3. Matulevicius, E., "Thermal Stratification in Enclosed Fluids Due to Natural Convection," Ph.D. Thesis, Massachusetts Institute of Technology, 1970.
4. Schwind, R.G. and Vliet, G.C., "Observations and Interpretations of Natural Convection and Stratification in Vessels," 1964 Heat Transfer and Fluid Mechanics Institute, 1964, pp. 51-68.
5. Drake, F.M., "Transient Natural Convection Within Vertical Cylinders," Sc.D. Thesis, Massachusetts Institute of Technology, 1966.
6. Emery, A. and Chu, N.C., "Heat Transfer Across Vertical Layers," Journal of Heat Transfer, Vol. 87, 1965, pp. 110-116.
7. Gill, A.E., "The Boundary-Layer Regime for Convection in a Rectangular Cavity," Journal of Fluid Mechanics, Vol. 26, 1966, pp. 515-536.
8. Elder, J.W., "Laminar Free Convection in a Vertical Slot," Journal of Fluid Mechanics, Vol. 23, 1965, pp. 77-98.

9. Krane, R.J., "The Solution of Laminar Natural Convection Flows in Rectangular Enclosures by the Method of Matched Asymptotic Expansions," Ph.D. Thesis, University of Oklahoma, 1972.

10. Sakurai, T. and Matsuda, T., "A Temperature Adjustment Process in a Boussinesq Fluid via a Buoyancy-Induced Meridional Circulation," Journal of Fluid Mechanics, Vol. 54, 1972, pp. 417-421.

11. Emmons, H.W., "Critique of Numerical Modeling of Fluid Mechanics Phenomena," Annual Review of Fluid Mechanics, Vol. 2, Sears, W.R., ed., Annual Reviews, Inc., Palo Alto, California, 1970, pp. 15-36.

12. Boussinesq, J., Theorie Analytique de la Chaleur, Vol. 2, Gathier-Villars, Paris, 1903.

13. Spiegel, E.A. and Veronis, G., "On the Boussinesq Approximation for a Compressible Fluid," Astrophysics Journal, Vol. 131, 1960, pp. 442-447.

14. Veronis, G., "The Analogy Between Rotating and Stratified Fluids," Annual Review of Fluid Mechanics, Vol. 2, Sears, W.R., ed., Annual Reviews, Inc., Palo Alto, California, 1970, pp. 37-66.

15. Greenspan, H.P., The Theory of Rotating Fluids, Cambridge University Press, Cambridge, 1969.

16. Trustrum, K., "Rotating and Stratified Fluid Flow," Journal of Fluid Mechanics, Vol. 19, 1964, pp. 415-432.

17. Doty, R.T. and Jischke, M.C., "Linearized Buoyant Motion due to an Impulsively Heated Vertical Plate," to be published.

18. Greenspan, H.P. and Howard, L.N., "On a Time Dependent Motion of a

Rotating Fluid," Journal of Fluid Mechanics, Vol. 17, 1963, pp. 385-404.

19. Greenspan, H.P., "On the General Theory of Contained Rotating Fluid Motions," Journal of Fluid Mechanics, Vol. 22, 1965, pp. 449-462.

20. Crabtree, L.F., Küchemann, D. and Sowerby, L., "Three-Dimensional Boundary Layers," Laminar Boundary Layers, Rosenhead, L., ed., Oxford University Press, London, 1963, pp. 409-417.

21. Hildebrand, F.B., Advanced Calculus for Applications, Prentice-Hall, Inc., Englewood Cliffs, New Jersey, 1962, pp. 451-454.

22. Rossby, C.G., "Relation Between Variations in the Intensity of the Zonal Circulation and the Atmosphere and the Displacements of the Semi-Permanent Centers of Action," Journal of Marine Research, Vol. 2, 1939, pp. 38-55.

23. Bishop, E.H., Mack, L.R. and Scanlan, J.A., "Heat Transfer by Natural Convection Between Concentric Spheres," International Journal of Heat and Mass Transfer, Vol. 9, 1966, pp. 649-662.

APPENDIX

LEIBNITZ'S RULE FOR THE CROSS PLANE

Let R be some three-dimensional region which varies with time, t. This region is bounded by the closed surface, S. Let S have an outward unit normal vector, $\hat{n}$, and velocity, $\vec{V}$. Then, for any scalar quantity, Q, Leibnitz's rule for differentiating an integral with variable limits is

$$\frac{d}{dt}\iiint_{R(t)} Q(\vec{r},t)d\tau = \iiint_{R(t)} \frac{\partial Q}{\partial t}\, d\tau + \oiint_{S(t)} Q\vec{V}\cdot\hat{n}ds \qquad (A.1)$$

where $\vec{r}$ is the position vector and $d\tau$ and dS are the differential elements of volume and surface area respectively.

In order to specialize this result to our case of flow in the cross plane, we take for our "region" the cross-plane area, A, which depends on the vertical spatial coordinate, z, as shown in Figure (A.1). Here, the area, A, is bounded by $\mathcal{C}$ with outward unit normal vector $\hat{n}^*$ in the plane of A. As the area changes from $A(z_1)$ to $A(z_2)$, $\mathcal{C}$ has a "velocity" $\vec{V}^*$ that is given by

$$\vec{V}^* = \frac{dx}{dz}\hat{e}_x + \frac{dy}{dz}\hat{e}_y \qquad (A.2)$$

as also shown in the figure.

As a "visual" aid, we may think of our region as being a rigid vertical cylinder of height h and base A(z), where Q does not vary over the height of any particular cylinder. This does not say that Q is invariant in z, but rather that Q varies in z as the base area, A, changes. This produces a different rigid cylinder over whose height Q does not vary. This rigid cylinder concept is shown in Figure (A.2).

The conventional form of Leibnitz's rule may be applied directly to this artificial region and the result is

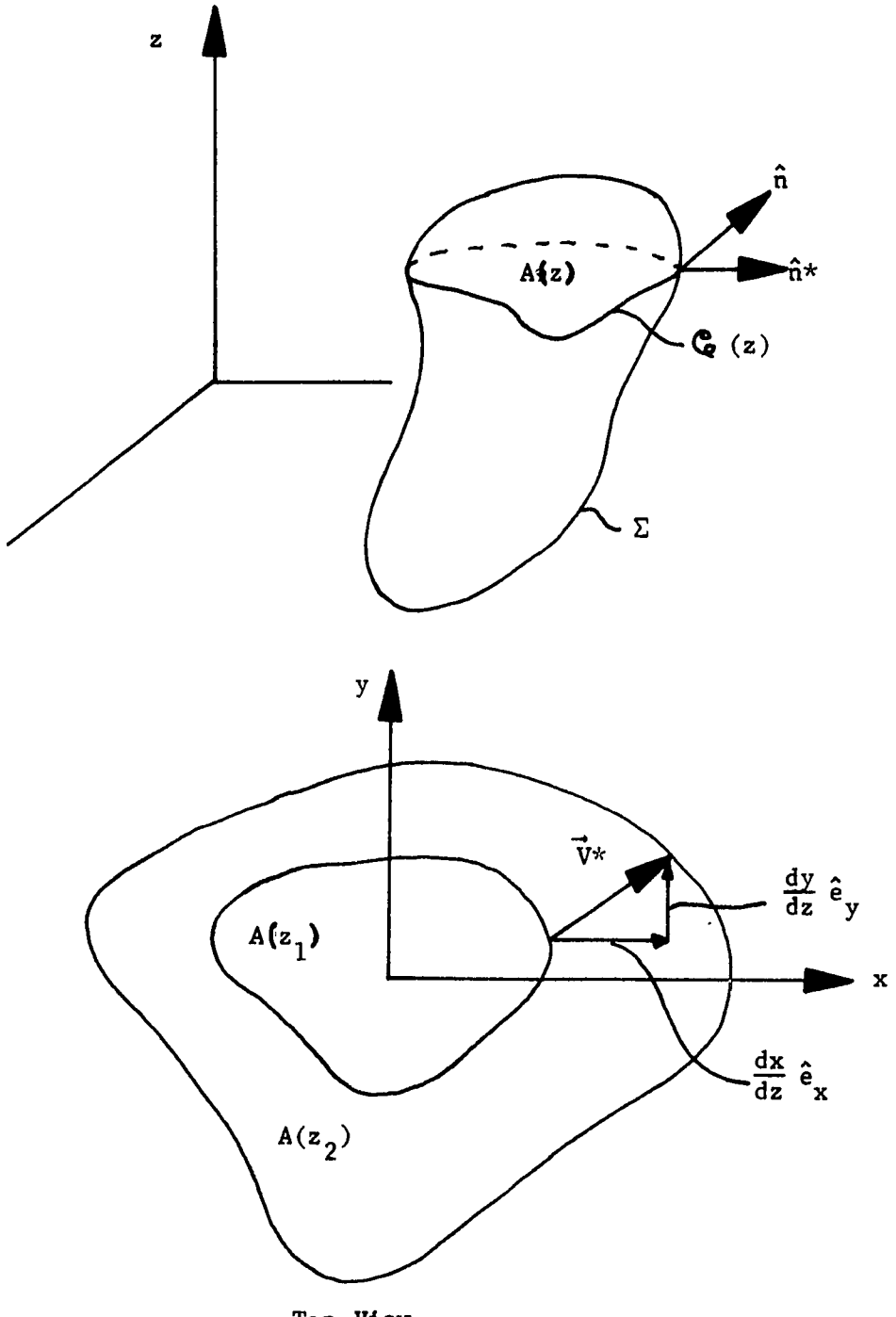

Figure A.1 Cross-Plane Geometry

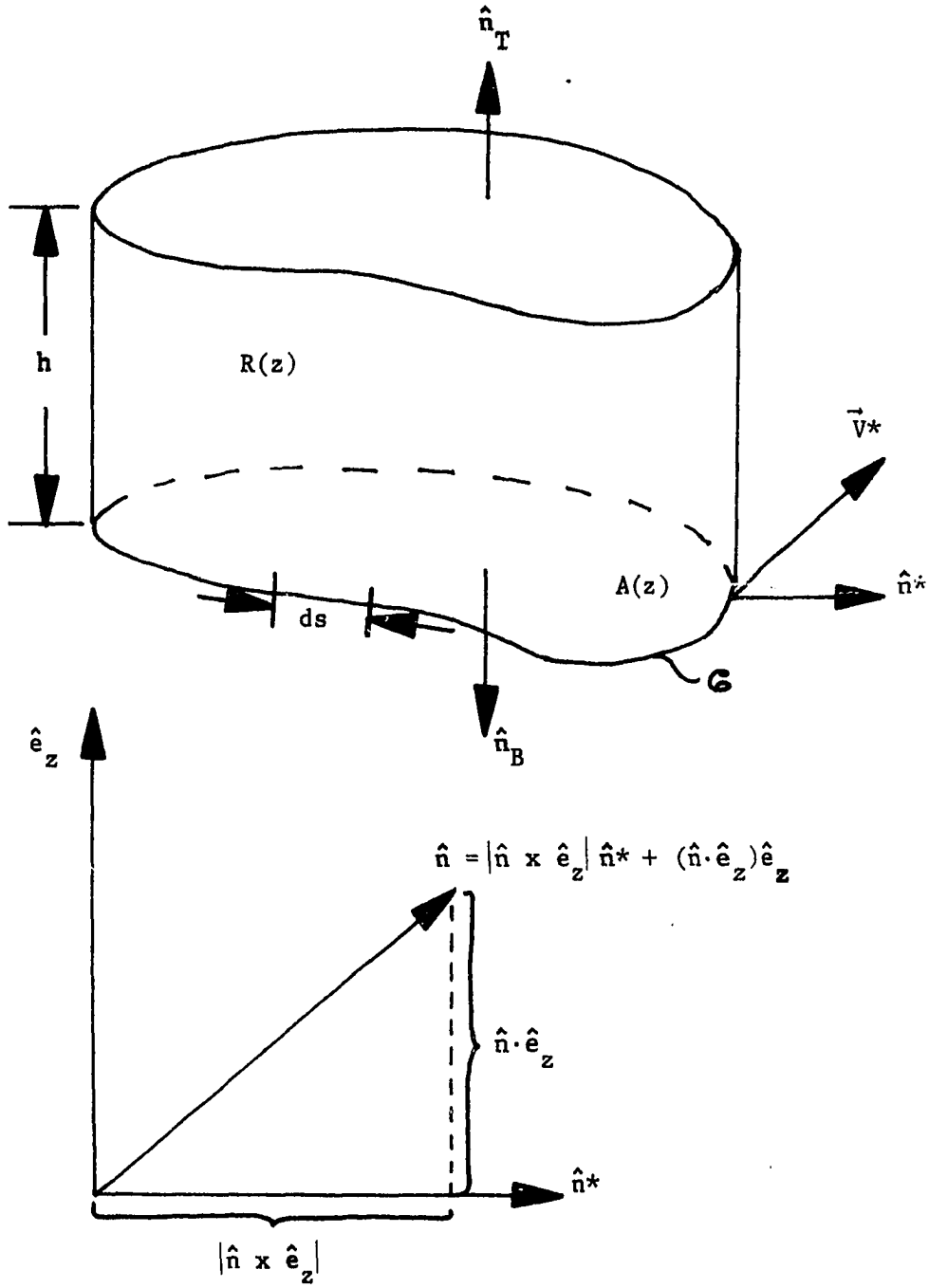

Figure A.2 Rigid Cylinder and Unit Normals

$$\frac{d}{dz}\iiint_{R(z)} Q(x,y;z)d\tau = \iiint_{R(z)} \frac{\partial Q}{\partial z}\, d\tau + \iint_{S(z)} Q\,\vec{V}^* \cdot \hat{n}\, dS \quad . \tag{A.3}$$

The integration over the region is equivalent to the product of the height of the cylinder with an integration over the base area. The integration over the surface may be broken into the sum of integrations over the side, top and bottom of the cylinder. The result of this integration is

$$h\frac{d}{dz}\iint_{A(z)} Q\, dA = h\iint_{A(z)} \frac{\partial Q}{\partial z}\, dA + h\oint_{\mathcal{C}(z)} Q\,\vec{V}^*\cdot\hat{n}^* ds$$

$$+ \iint_{A(z)} Q\,\vec{V}^*\cdot\hat{n}_T dA + \iint_{A(z)} Q\,\vec{V}^*\cdot\hat{n}_B\, dA \quad . \tag{A.4}$$

But $\hat{n}_B = -\hat{n}_T$ and consequently the last two integrations cancel leaving

$$\frac{d}{dz}\iint_{A(z)} Q\, dA = \iint_{A(z)} \frac{\partial Q}{\partial Z}\, dA + \oint_{\mathcal{C}(z)} Q\,\vec{V}^*\cdot\hat{n} ds \quad . \tag{A.5}$$

Let the container, Σ, be described by a function, F, such that

$$F(x,y,z) = z - f(x,y) = 0 \quad \text{on } \Sigma \tag{A.6}$$

This equation implies the relationship

$$\nabla F = \hat{e}_z - \nabla f \tag{A.7}$$

which may be coupled with the total derivative

$$\frac{dF}{dz} = \frac{\partial F}{\partial x}\frac{dx}{dz} + \frac{\partial F}{\partial y}\frac{dy}{dz} + \frac{\partial F}{\partial z} = 0 \text{ on } \Sigma \tag{A.8}$$

to yield

$$-\nabla f \cdot \vec{V}^* + 1 = 0 \quad \text{on } \Sigma \tag{A.9}$$

by making use of Eq. (A.2) for $\vec{V}^*$ and noticing that $\partial F/\partial z$ is unity from Eq. (A.6). The outward unit normal to the container is $\nabla F/|\nabla F|$, which can be related to the unit normal in the cross plane, as shown in Figure (A.2), as follows

$$\hat{n} = \frac{\nabla F}{|\nabla F|} = \frac{\hat{e}_z - \nabla f}{\sqrt{1 + (\nabla f)^2}}$$

$$= |\hat{n} \times \hat{e}_z| \hat{n}^* + (\hat{n} \cdot \hat{e}_z)\hat{e}_z \quad . \tag{A.10}$$

Solving this for ∇f we obtain

$$\nabla f = - \frac{|\hat{n} \times \hat{e}_z|}{(\hat{n} \cdot \hat{e}_z)} \hat{n}^* \tag{A.11}$$

where we have used the fact that

$$\hat{n} \cdot \hat{e}_z = \frac{1}{\sqrt{1 + (\nabla f)^2}} \quad . \tag{A.12}$$

The latter result can be obtained by inspecting Eq. (A.10), keeping in mind that ∇f has no component in the z-direction.

We may now substitute for ∇f from Eq. (A.11) into Eq. (A.9) to obtain

$$\vec{V}^* \cdot \hat{n}^* = - \frac{\hat{n} \cdot \hat{e}_z}{|\hat{n} \times \hat{e}_z|} \quad . \tag{A.13}$$

With this, Leibnitz's rule, as modified for the cross plane, may be written from Eq. (A.5) as

$$\frac{d}{dz} \iint_{A(z)} Q \, dA = \iint_{A(z)} \frac{\partial Q}{\partial z} \, dA + \oint_{\mathcal{C}(z)} Q \left(- \frac{\hat{n} \cdot \hat{e}_z}{|\hat{n} \times \hat{e}_z|} \right) ds \quad . \tag{A.14}$$

It is of interest to set Q to unity in this expression and obtain the result

$$\frac{dA}{dz} = \oint_{\mathcal{C}} \left(- \frac{\hat{n} \cdot \hat{e}_z}{|\hat{n} x \hat{e}_z|} \right) ds \quad . \tag{A.15}$$

This result is used in the heat-up analysis in going from Eq. (3.39) to Eq. (3.41).